Feasibility Study on the use of Nickel and Cobalt as Filler Material in Smart Isotropic MR Elastomers

FINAL YEAR PROJECT UG 2017

By

Behram Khan Mahsud	00000 212593
Umer Majid	00000 211303
Jahanzaib Shahzad	00000 210065
Muhammad Talha Abid	00000 209755

NUST Institute of Civil Engineering (NICE)

School of Civil and Environmental Engineering (SCEE)

National University of Science and Technology (NUST), Islamabad, Pakistan

2021

This is to certify that the Final Year Project Titled

"Feasibility Study on the use of Nickel and Cobalt as Filler Material in Smart Isotropic MR Elastomers"

Submitted By

Behram Khan Mahsud	00000 212593
Umer Majid	00000 211303
Jahanzaib Shahzad	00000 210065
Muhammad Talha Abid	00000 209755

has been accepted towards the requirements for the undergraduate degree

in

CIVIL ENGINEERING

Dr. Muhammad Usman
Structural Engineering
Department NUST Institute of
Civil Engineering

School of Civil and Environmental Engineering National University of Sciences and Technology, Islamabad.

DEDICATION

To our beloved parents, teachers, mentors and colleagues who have stood by our side in rough and tough times, who have taught us to show perseverancein the face of adversity.

ACKNOWLEDGEMENTS

In the name of Allah, the most Beneficent, the most Merciful as well as peace and blessings upon Prophet Muhammad, His servant and final messenger.

First of all, we would like to thank our Creator ALLAH to have given us the chance to perform this research. He has guided us through each and every step of difficulties faced in carrying out the research work.

We are also greatly thankful to our parents who have supported us through every thick and thin of our life's journey. They have supported us when we were not able to walk, and they are still supporting us to continue and provide solutions for humanity.

We are also obliged from the depths of our hearts to pay special thanks to attributing to our supervisor Dr. Muhammad Usman. He has helped us in every part of our thesis and has also provided us with great ideas, tips, and tricks to solve problems, whether they were in the software or performing physical experimentation tasks. We feel the responsibility to thank him for his patience, guidance, and cooperation throughout the FYP. We are also extremely grateful to Ms. Sadia Umer Khayyam. Her research work has helped us a lot. She worked on Development and characterization of a novel hybrid magnetorheological elastomer incorporating micro and nano size iron fillers.

We value the assistance provided by the entire staff of Structures Lab, NICE. We would also like to mention Faculty of National Textile University (NTU), Faisalabad, for their cooperation and making the testing machine available for us.

Finally, we would pay our gratitude and mention to all who have participated knowing and unknowingly to assist to our study.

ABSTRACT

Inspired and benefited by its controllable and field-dependent stiffness/damping properties, there has been an increasing research and development on magnetorheological elastomer (MRE) for mitigation of unwanted structural or machinery vibrations using MRE isolators or absorbers. The main aim of this research work was to determine the behaviour of MRE using Nickel and Cobalt and to compare the magnetorheological effect between them. Most of the research work have been done on MREs using carbonyl iron as filler material, so this study aimed at observing any change in characteristics of MREs using Nickel and Cobalt as filler particles. The use of nickel and cobalt has been increasing in magnetic appliances in every field and their magnetic properties at micro level are almost similar to carbonyl iron. So, the CI particles were replaced with Ni and Co particles. The research work methodology comprised of characterization of metallic powders to determine size of particles and check for impurities, then casting was done following it was the micro-image analysis of casted MREs and then the dynamic shear testing on the casted samples and finally the analysis of obtained results. The outcome of this research work was that for Nickel and Cobalt higher MR effect was observed at lower filler percentages and also higher MR effect was observed for Nickel based MREs than for Cobalt based MREs.

TABLE OF CONTENTS

Contents

LIST OF FIGURES

LIST OF TABLES

CHAPTER 1: INTRODUCTION

1.1 General:

Earthquake is the shaking and vibration at the surface of the earth resulting from the underground movement along a fault plane or from the volcanic activity. Pakistan geologically overlaps both the Eurasian and Indian tectonic plates. Seismic activity in this region is a result of collision between the two plates. Due to this seismic activity, Pakistan has been under continuous threats and devastations of the earthquake. Several major earthquakes including the 2005 Kashmir, Balakot earthquake which was the toughest and the most distressing one have damaged the infrastructure of Pakistan including more than a million buildings. So, in order to negate the effect of these earthquakes, structures resistant to such shakings and vibrations should be built. Recent advancements in the field of civil engineering have made it possible to protect the structure from earthquake forces. Many techniques have been in use and base isolation technique using smart materials is now catching the attention.

1.2 Base Isolation:

“Base isolation” is a technique that separates the structure and its components from the dangerous earthquake ground motion Base isolation is achieved by mounting the superstructure on the system of supports that are stiff and strong with respect to vertical forces and are showing low stiffness in the horizontal direction. The main purpose of base isolation is to reduce the story drifts and floor accelerations to protect not only the structure but also its contents from damage. This technique works by deflecting and dissipating the seismic energy, lowering the natural frequency, and increasing the time period of the structure. In this way, base isolation minimizes the acceleration response and amplitude of the horizontal movement of the structure and protects its structural integrity. Conventional base isolators come under the category of passive vibration control systems. These passive base isolators are vulnerable against the strong ground motions generated at the near-fault and far-fault locations. So, to overcome the issues faced by the passive base isolators many researches and modifications have been done in order to get more efficient base isolators for buildings and bridges. There are several systems that are capable of reducing the seismic demand of the structure which includes elastomeric rubber bearings, ball bearings, roller bearings, and springs.

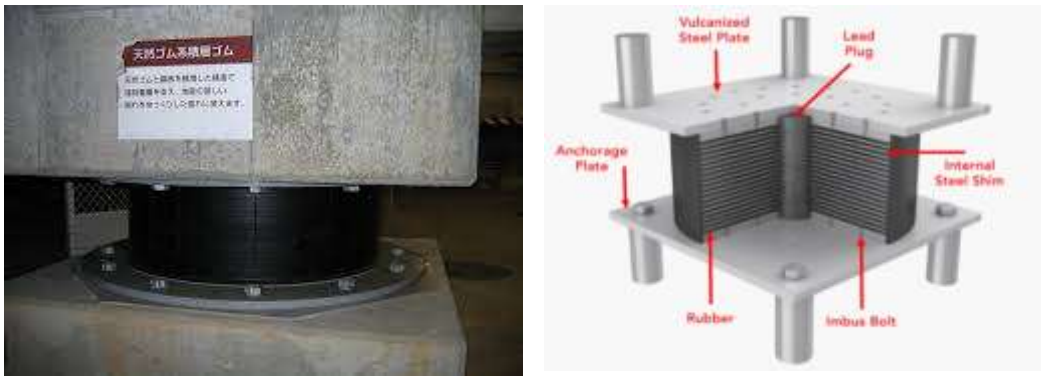

Figure 1. 1*: Base Isolator and its section view showing layers of steel and elastomers.*

1.3 Magnetorheological Elastomers:

Magneto-rheological (MR) materials belong to a category of so-called smart materials whose rheological properties can be modified by an externally applied magnetic field. There are two broad categories of MR materials MRFs (Magneto-rheological Fluids) and MREs (Magneto-rheological Elastomers). In MR fluids, magnetic particles are suspended in a non-magnetic fluid such as silicon oil, and these fluids are known for large stress enhancement. Initially, MR fluid base isolators were used to overcome the issues related to the conventional base isolators. But there are some flaws like contamination of the environment, sedimentation of particles due to large density mismatch in MR Fluids. So, to address these issues MR Elastomers were introduced in order to counter the drawbacks of MR Fluids. MR elastomers are composed of micro-sized ferromagnetic particles dispersed in an elastomeric matrix. The distribution of magnetic particles in the elastomer can be either homogenous (isotropic) in the absence of an external magnetic field or a chain-like structure (anisotropic) in the presence of an external magnetic field during the curing process. The ability of MR elastomers to adjust their stiffness or rigidity under the wide range of magnetic field, loading frequency, and amplitude has made them a suitable candidate material to be used as a basic material to develop seismic base isolators for civil engineering applications. The results of the recent researches have also shown that the suggested system has the ability to surpass the conventional method of reducing the responses of the structures during earthquakes.

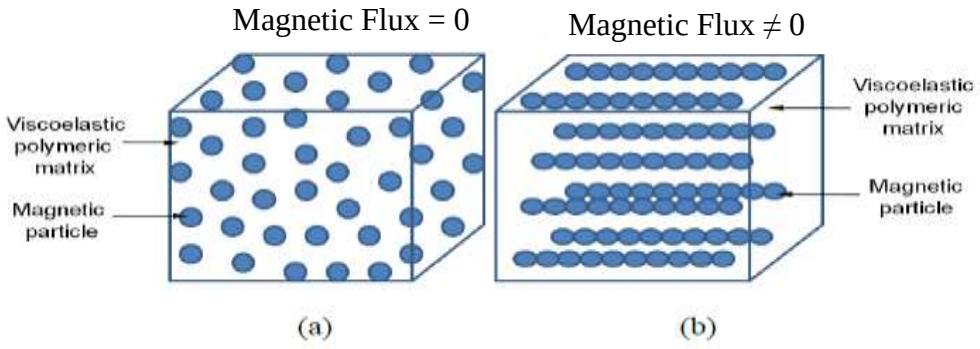

Figure 1. 2: *Schematic of MREs (a) Isotropic (b) An-Isotropic*

1.4 Application of MREs:

There are many engineering applications MREs such as:

- Vibration absorbers.
- Base Isolators.
- Vibration Dampers.
- Actuators for valves.

1.5 Problem Statement:

This research will develop mechanisms and alternatives for existing materials and practices in order to bring an improvement to the structural integrity of structures. Many studies have been done on MRE using carbonyl iron as a filler material. So, there is a need to find the alternative of carbonyl iron (ferromagnetic material) to use in MRE as a filler material.

1.6 Objective:

The objective of this research is:

- To study the effect of using micro sized Nickel and Cobalt particles as filler materials on the dynamic shear properties of Magnetorheological Elastomers.
- To study the Magnetorheological Effect of MRE using different ratios of filler particles under Shear Loading.
- To compare the Magnetorheological Effect between the MREs reinforced with Nickel and Cobalt.

1.7 Scope of Work:

The main aim of this research work is to determine the behaviour of MRE using Nickel and Cobalt and to compare the magnetorheological effect between them. Most of the research work has been done on MREs using carbonyl iron as filler material, so we aimed at observing any change in characteristics of MREs using Nickel and Cobalt as filler particles. The use of nickel and cobalt has been increasing in magnetic appliances in every field and their magnetic properties at the micro level are almost similar to carbonyl iron. So, we replace the CI with Ni and Co particles.

1.8 Thesis Layout:

A brief introduction of research is presented in 1st chapter of this thesis which describes the background, aims and scope of research. 2nd chapter contains literature review on MREs, 3rd chapter discusses about the materials and equipment used, 4th chapter discusses methodology used for the preparation of samples, experimental work is summed up in 5th chapter, 6th chapter deals with discussion on results and 7th chapter provides conclusions and recommendations.

CHAPTER 2: LITERATURE REVIEW

2.1 MRE:

It is a device to use as base isolators in the event of an earthquake overcome the destructive vibration and forces of earthquake. Recently, MRF (Magnetorheological fluids) isolators have also been used, but MRF has shortcomings of their own, in order to address those shortcomings this device was made. Some of the disadvantages of using MRF are particle deposition, environmental contamination, and capability of being only One DOF system etc., due to these issues it was replaced by MRE (Magnetorheological Elastomers) [1]. The property of a substance to change its stiffness when magnetic field is applied is known as Magnetorheological effect [2]. MRE are included in the category of smart materials [3,4].

2.2 MRE composition:

MRE are composed of mainly two types of material; a ferromagnetic filler which is magnetically polarizable and a non-ferromagnetic matrix [5]. The ratio of each mixing material is dependent on the stiffness, hardness and curing of the sample. After curing the ferromagnetic material have a fixed position in the material. After the magnetic field is applied the particles re-align to form a chain-alike structure, that changes the mechanical properties of the material [6,7]. This type of effect is also present by changing the stiffness [8]. Researchers have used different kind of materials Graphene Nano particles, Fe nanowires and Nickel [9,10,11].

2.3 Matrix material:

The usual rubber matrix material used are silicone rubber [12], polybutadiene rubber [13], nitrile rubber[14], and polyurethane (PU)[15]. Due to this solid matrix material MRE are referred to as solid state magnetorheological fluids [16,17]. Selection of matrix material drastically affects the production of MRE for research purposes [9]. Matrix material also significantly affects the thermal stability of MRE [9]. Temperature dependent nature of MRE is due to thermal properties of the matrix elastomer [18].

2.4 Filler Particles:

Other than the matrix, the other composite used in the MRE is filler particles, most common filler used is carbonyl iron [23] because it matches the requirement of fast de-magnetization meaning there will be less magnetic effect retained by the material whenever magnetic field is removed. It also passes the requirement of high permeability, that is magnetization of a material under applied magnetic field. These two properties combined increases the particles interaction with matrix material [5,18-20].

2.5 Content of Filler particles:

In previous researches, it was shown that using filler content enhances the MR effect and reinforces it [5]. Higher filler content also (specifically iron) results in larger ratio of flux density to field density [21]. It has been noted that with increased amount of filler ultimate strengths have increased provided that filler diameter used is small [22]. With 1-9μm 25-30% of filler particle produces ideal MR effect [23]. Also, by Von Lockette, using filler content 30-40% can increase stiffness up to 50% [24]. A higher content of carbonyl iron particle can increase the initial stiffness modulus (i.e., the stiffness without magnetic field) but not the MR effect.

2.6 Additives:

With the matrix material and filler particles different other materials are also used to enhance the properties of MRE, among the list are, silicone oil, graphite powder and micro metal powders to enhance the mechanical as well as chemical properties of MR elastomer [25]. With the addition of Silicone Oil, it was noted SO disperses fillers well without agglomeration [26]. A researcher has also used Carbon nanotubes as an additive, it proved to increase the dynamic stiffness, it increased by 37% [36]. The addition of gamma-ferrite additive in CI/NR composite elastomer resulted in higher modulus in strain sweep test [37].

2.7 MRE testing:

The mechanical properties of magnetorheological elastomer can be characterized by using dynamic test, for this a variety of parameters and modes can be selected [27,28]. Earthquake forces are most of the time in shear mode, reason being for the testing of MRE in shear mode [27]. These tests and modes are categorized by displacement direction (direction of force) and the applied magnetic field direction, if the magnetic field applied with the help of any source

is parallel to the displacement of the MRE, then it is in squeeze mode and if it is perpendicular, then the mode is called Shear mode [29]. Increasing of elastic Moduli with increasing strain rate and flux was observed. Furthermore, testing is also performed with on less strain amplitudes with the range of 1 - 50% of strain [30,31].

2.8 Particle Shape and Size in MRE:

Particle size is distribution is very important to characterize the MRE. In a paper published by Q Jin [32], influence of particle size on rheology of MRE is studied, it was concluded, samples with smaller dia particles had larger initial shear modulus (i.e., without application of magnetic field) and with larger dia showed smaller initial shear modulus.

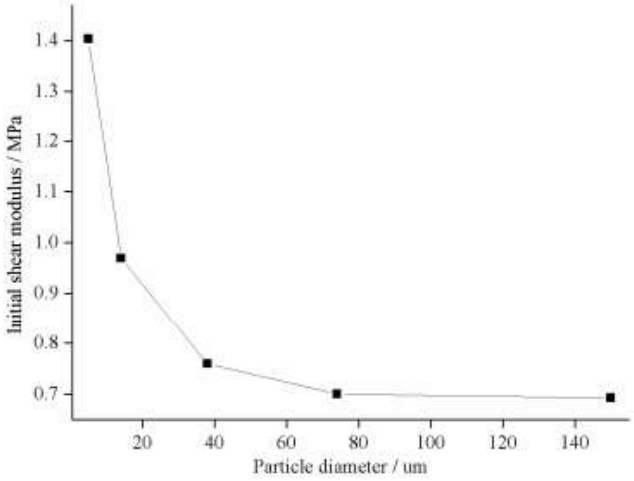

***Figure 2. 1**: Initial Shear Modulus of MRE samples with different diameter particles [35].*

In a research published by J. Winger [33], dependence between size fraction and magnetorheological effect was found to be a factor of two. The effect of shape and volume fraction was also observed by C. Sarkar [34], Large sized particles with low volume fraction with flaky shapes perform better at low shear rates, whereas, at moderate shear rates, large sized particles at low volume fraction perform better as compared to 'small sized' and 'mixed size' particles. At moderate volume fraction, best results were obtained by 'mixed size' particles. Although with the increase in volume fraction, 'mixed size' particles show the best performance. Approaches for hybrid mixtures of nano and micro sized fillers has also been made [5], It was seen that instead of using micro or nano fillers has a whole produced less MR effect than using materials in conjunction with each other. A stiffness increases of up to 40% was reported as compared to initial state modulus. Demchuk showed that magnetorheological

elastomer with particle size less 3µm showed less magnetizing effect as compared to particles with 13µm, researcher recommend using a size of greater than 3µm [35].

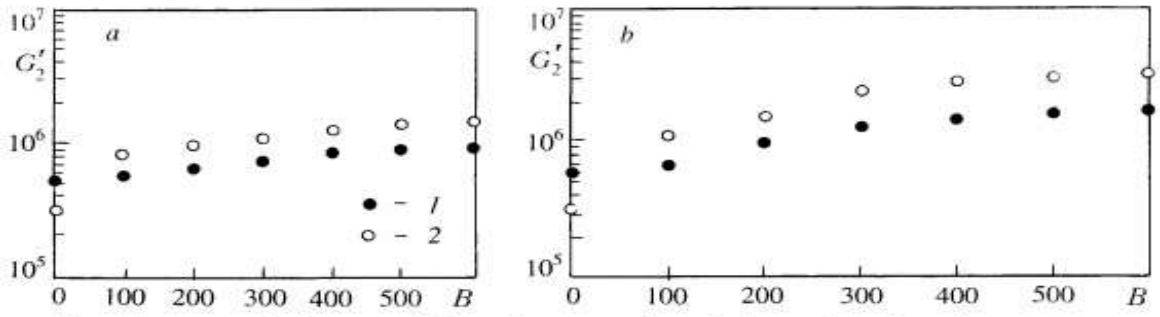

Fig. 3. Accumulation modulus of an unoriented formoplast-based magnetorheological elastomer (a) and of an oriented one (b) vs. magnetic field intensity: 1) particle diameter is 3.5 and 2) 13 µm.

Figure 2. 2: *Accumulation modulus of and unoriented formoplast-based magnetorheological elastomer (a) and of an oriented one (b) vs. magnetic field.*

(1) Particle dia 3.5µm (2) 13µm [35].

2.9 Research Gap:

It can be concluded that MRE's are a vast field and despite the previous research, a lot of work is needed to be done. Perhaps, the most important research topic may be the 'Design of MRE', No formal procedure is present for the design, we may understand of how the MRE may work but the knowledge required to predict the performance of MRE is still less. One other research area is by changing the filler material and moving away from carbonyl iron and finding more alternatives, that are cheap to produce and simultaneously feasible.

CHAPTER 3: MATERIAL & EQUIPMENTS

3.1 Cobalt and Nickel particles:

The percentage of nickel and cobalt filler particles as shown in Table 3.1 were decided on basis of trial. As the MREs at higher percentage were very rough on the surface and stiff as can be seen in Figure 3.1 so after the new percentages that were selected are shown in Table 3.2 shows that MREs obtained with these percentages gave better smooth surface and were soft on pressing as can be observed in Figure 3.2.

Table 3. 1: *Percentages of Cobalt and Nickel Powder*

Sr. No.	Particles Percentages	
	Cobalt (%)	Nickel (%)
1.	5	5
2.	10	10
3.	15	15

Figure 3. 1*: MRE Sample at 15% Filler Content*

Table 3. 2: *Percentages of Cobalt and Nickel Powder*

Sr. No.	Particles Percentages	
	Cobalt (%)	Nickel (%)
1.	2.5	-
2.	5	5
3.	7.5	7.5
4.	10	10

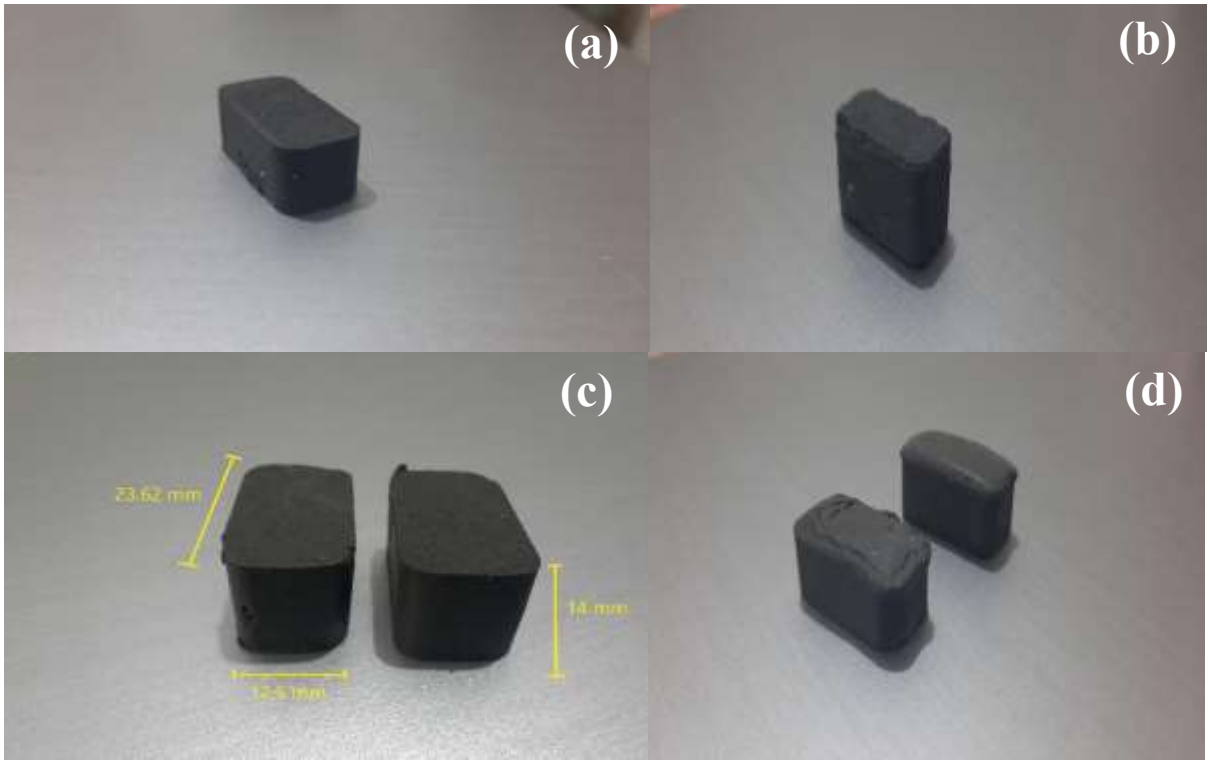

Figure 3. 2*: MRE Samples (a) Nickel 5% (b) Cobalt 5% (c) Nickel 10%*

3.2 Silicon Rubber and Silicon Oil:

The silicon elastomer has more advantage over conventional rubber matrix, moreover magnetorheological phenomena is more prominent in silicon elastomers. Silicon oil as an additive is added in elastomer matrix to increase Magnetorheological effect by making a soft MRE. Figure 3.3 shows that silicon elastomer was imported from Shenzhen Rongxingda Polymer Material Co., Ltd. from China through Alibaba to use in MRE as matrix material, it has two parts (part A and part B) to be mixed in 1:1. Silicon oil was imported from Miingcheng Group Ltd. Dongguan, Gaung Dong, China as an additive in MRE. Properties of Silicon Elastomer and Silicon oil are shown in Table 3.3 and Table 3.4, respectively.

Table 3. 3: *Parameters of Silicon Elastomer*

Translucent Silicone (A:B = 1:1)		
Sr. No.	**Parameter**	**Value**
1.	Hardness	5 +/- 2 Shore A
2.	Tensile Strength	>=2.5 Mpa
3.	Viscosity	5000 +/- 500 mPas
4.	Elongation	>=550%

5.	Shrinkage Rate	<0.1%
6.	Tear Strength	>12 MPa
7.	Pot Life	30-40 mins
8.	Curing Time	3-5h

Table 3. 4: *Parameters of Silicon Oil*

Sr. No	Parameter	Value
1	Item No.	MC-100
2	Vapor density	<1 (vs. Air)
3	Vapor Pressure	<5 mmHg (25 °C)
4	Viscosity	100 cSt (25 °C)
5	Density	0.96 g/ml at 25 °C

Figure 3. 3: *Silicon Rubber (Part A & B) and Silicon Oil*

3.3 Electronic Top Loading Balance:

Digital weighing balance was used to measure weights of materials less than 1kg. The specifications of weighing balance are as following:

Table 3. 5: *Parameters of Digital Weighing balance*

Sr. No	Parameter	Value
1.	Model no.	321-64503-72
2.	Capacity	620 carats
3.	Brand Name	Shimadzu
4.	Temperature range	5/40°C

Figure 3. 4*: Electronic Loading Balance*

3.4 Ultrasonic bath Sonicator:

An ultrasonic bath Sonicator as can be seen in Figure 3.5 is used for homogeneous mixing, de-agglomerating and dispersing of nanoparticles. Parameters are shown in Table 3.6. It digitally displays temperature and timer.

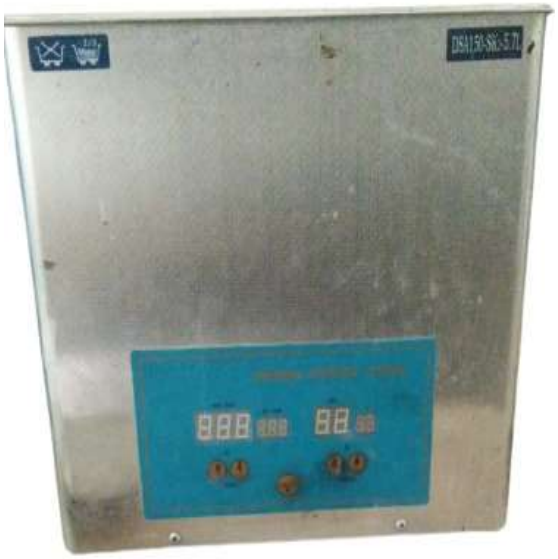

Figure 3. 5: *Ultra-Sonic Bath Sonicator*

Table 3. 6: *Parameters of Sonicator*

Sr. No.	Parameter	Value
1	Model no.	DSA150-SK2
2	Capacity	5.7 L
3	Material	Stainless steel
4	Temperature	60 °C
5	Frequency	20kHz

3.5 Steel Mold:

A steel mold consisting of two plates was prepared for the casting of MRE samples. The thickness of both plates was kept 14 mm, one plate consisting of rectangular and square slots

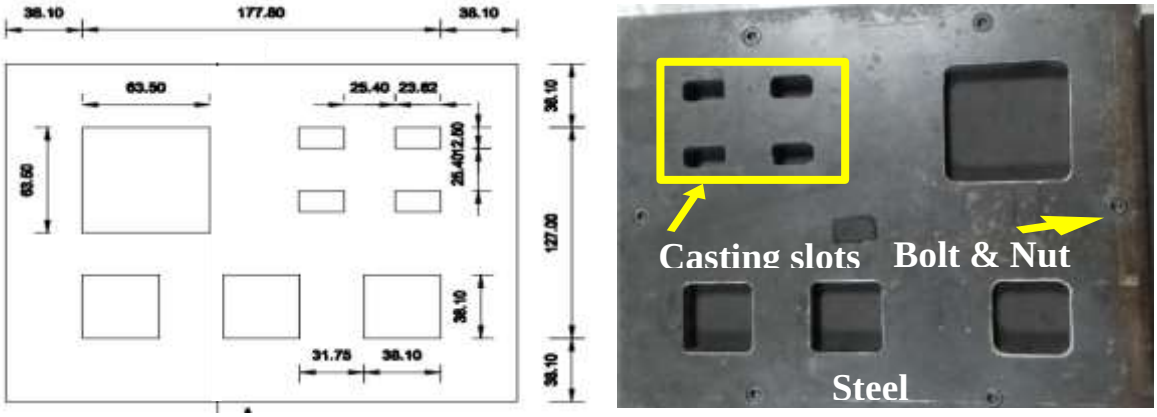

Figure 3. 6: *Steel Mold and its Plan View*

of different sizes were fixed with bolts and nuts above the other plate, which serve as a base of mold. The dimensions of different slots are mentioned in Figure 3.6.

3.6 Permanent Magnets:

Pair of Permanent Neodymium magnets were imported from China through importers/traders/wholesalers Fair Deal Enterprises, Lahore, Pakistan. These magnets were used to test field-dependent properties of MRE. The properties of Magnets are mentioned in table 3.7.

Table 3. 7: *Parameters of Permanent magnets*

Sr. No	Parameter	Value
1.	Grade No.	N52
2.	Size	50x50x40 mm
3.	Coating	Nickel
4.	Tolerance	+/- 0.5 -1mm
5.	Max. Working temperature	80 °C
6.	Gauss Power	5500+/-100

3.7 Gauss Meter:

Gauss meter as shown in figure 3.7 is a digital display meter for the measurement of electromagnetic wave in Gauss (G), miliGauss (mG), miliTesla (mT) or microTesla (μT) units having technical parameters mentioned in table 3.8. Magnetic flux values were measured physically during experiment at different distances on design assembly, in such a way that two points on top and bottom, and one at the middle was selected on sample parallel to the line C-D (figure 4.2) and for each point three readings were observed for averaging using Gauss meter, same technique was used for line parallel to A-B.

Table 3. 8: *Parameters of Gauss Meter*

Sr. No	Parameter	Value
1.	Model	DX-102
2.	Minimum Resolution	0.1mT
3.	Accuracy	Better than 1% (+/- 1000mT) Better than 2% (1000mT +/– 2000mT) Better than 3% (2000 mT +/- 3000mT)
4.	Gauss Range	30mT, 300mT, 3000mT three gears

Figure 3. 7*: Gauss Meter*

CHAPTER: 4 METHODOLOGY

The methodology for experiment involves preparation of design assembly for performing test, preparation of samples, characterization of samples and determining properties of samples.

4.1 Design Assembly

For dynamic test the assembly used was the same as prepared by Sadia Umer Khayyam [1] using FEMM software, the results of which are shown in table 4.1. The samples were glued to

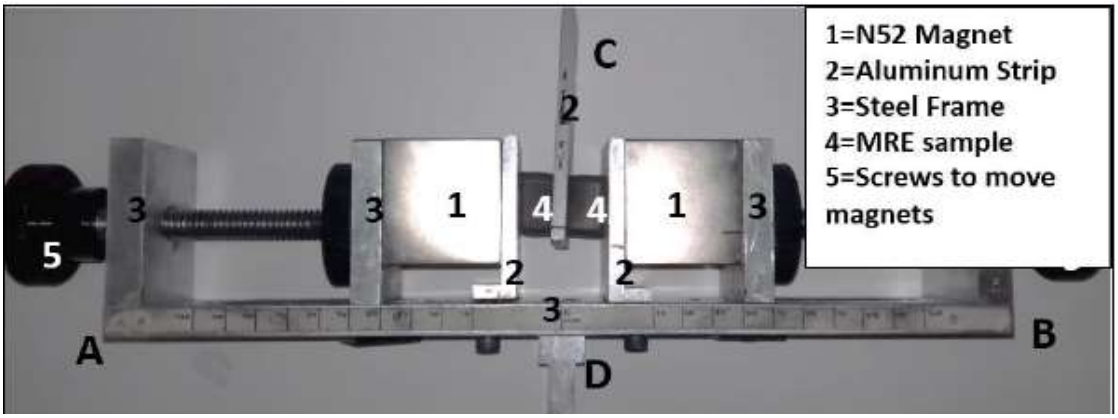

Figure 4. 1: *Design Assembly for MRE testing with a MRE samples and Permanent Magnets [5]*

L shaped aluminum strips using a strong glue and then the aluminum strips along with glued samples were screwed to the apparatus at its appropriate place. A straight aluminum strip was also introduced between the two elastomeric samples with its free end extruding so it can be clamped with the upper moveable jaw of the cyclic loading machine, the samples were also attached to it using glue. Aluminum was introduced so to concentrate the magnetic field lines in MRE samples as aluminum is a non-magnetic material.

4.2 Finite Element Magnetic Model

Finite Element Method Magnetics (FEMM) Software deals with electromagnetic problems. Software offers various tools to specify different parameters analyse them and provides suitable solution to suit our requirement. Figure 4.2, shows FEMM model of design assembly. The encircled red line parallel to line C-D in figure 4.2 is the line along which magnetic flux variation has been plotted in figure 4.3, the top of red line is 0 mm distance and bottom is 24 mm distance. Flux values were confirmed using FEMM software with only a 5.8 % maximum variation (Table4.1). FEMM analysis shows a decrease in flux values with an increase in

distance between magnets (line A-B) and an exponential decrease in flux from the centre to edges of elastomers across the assembly along the line C-D. (Figure 4.2).

Table 4. 1: *Comparison of Magnetic Flux Observed during Experimentation with FEMM Model Results [5]*

Case	Distance	Observed Magnetic Flux (Gauss Meter)	Magnetic flux from FEMM Model (Peak Value)	Difference
A	61 mm	0.4 T	0.388 T	-3%
B	67 mm	0.3 T	0.302 T	+0.2%
C	77 mm	0.2 T	0.215 T	+1.5%
D	87 mm	0.1 T	0.158 T	+5.8%

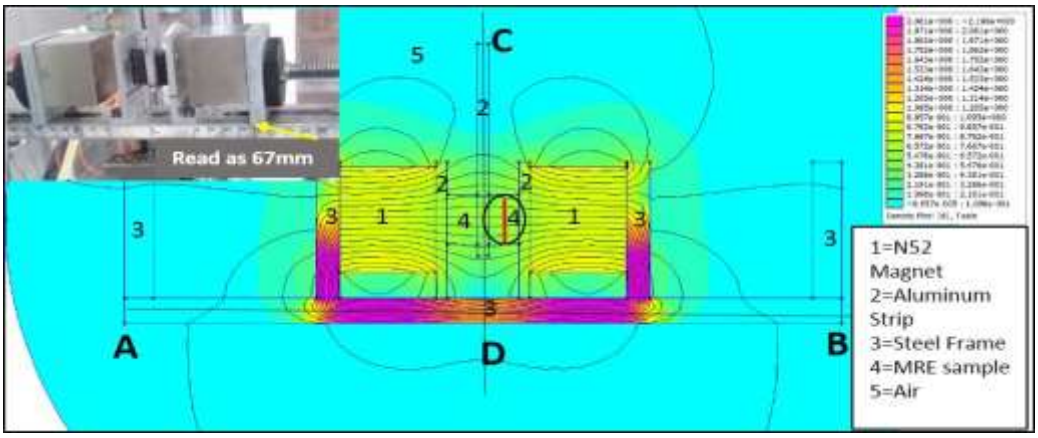

Figure 4. 2: *Distance between aluminium plate and face of magnet is 0 mm (61mm as per scale on assembly) [5].*

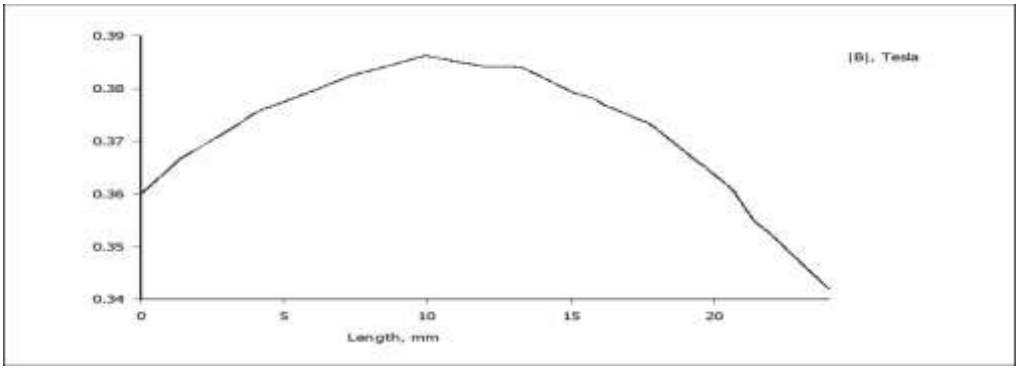

Figure 4. 3: *Magnetic Flux variation across line C-D [5].*

4.3 Preparation of particles:

The powdered particles were imported from an online material store in China named as "Hurricane Magnets & Materials" through Amazon and the images of the materials are as shown below, (These sample were discarded as it had interacted with air and their high chances of oxidation which could alter of experimental results).

***Figure 4. 4**: Cobalt powder*

***Figure 4. 5:** Nickel powder*

4.4 Characterization of Particles:

Characterization of magnetic particles was done to determine the particle size and morphology and to check the presence of any unwanted material in our powder material which could have worse effects on our results. The Characterization techniques performed were:

- PSA (Particle Size Analysis test)
- SEM (Scanning Electron Microscopy Test)
- EDS (Energy Dispersive Spectroscopy Test)

4.4.1 Particle Size Analyzer:

The size of Nickel and Cobalt particles were analysed using PSA (Horiba Laser Scattering Particle size distribution Analyzer LA-920) and the resulting graphs are as shown:

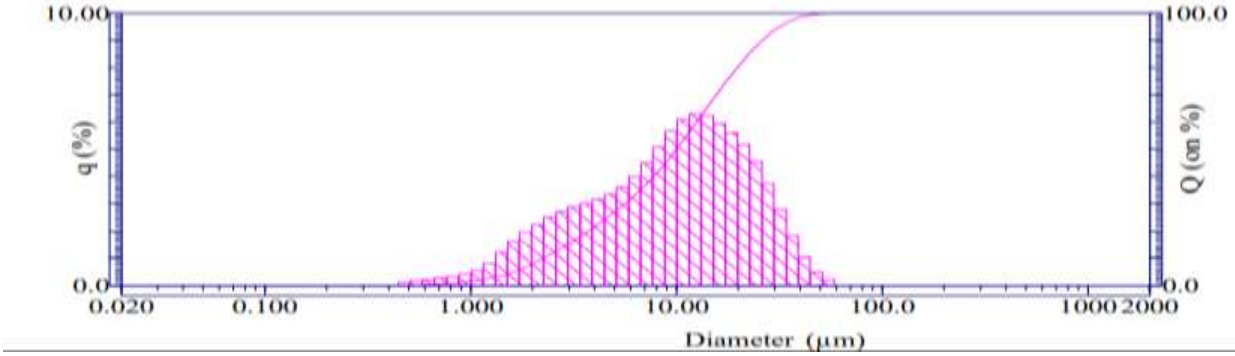

***Figure 4. 6**: Particle size analysis of nickel powder*

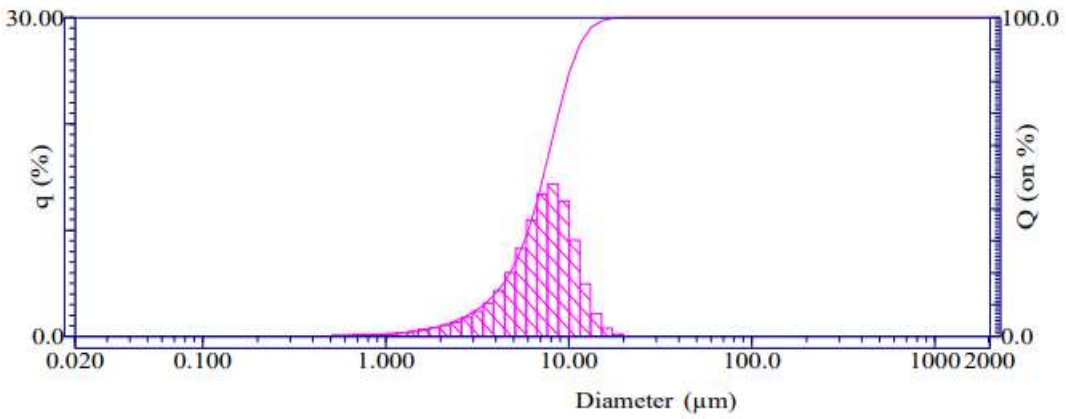

Figure 4. 7: *Particle size analysis of cobalt powder*

Graph for cumulative percentage passing and particle diameter was plotted to obtain mean sizes of nickel and cobalt and from the results of the analysis we can confirm that the particles sizes are in micro range which are 12.39µm and 7.35µm respectively.

4.4.2 Scanning electron microscope (SEM)

The size and morphology of as received cobalt and nickel particles was observed using SEM (JEOL JSM-6490A) images.

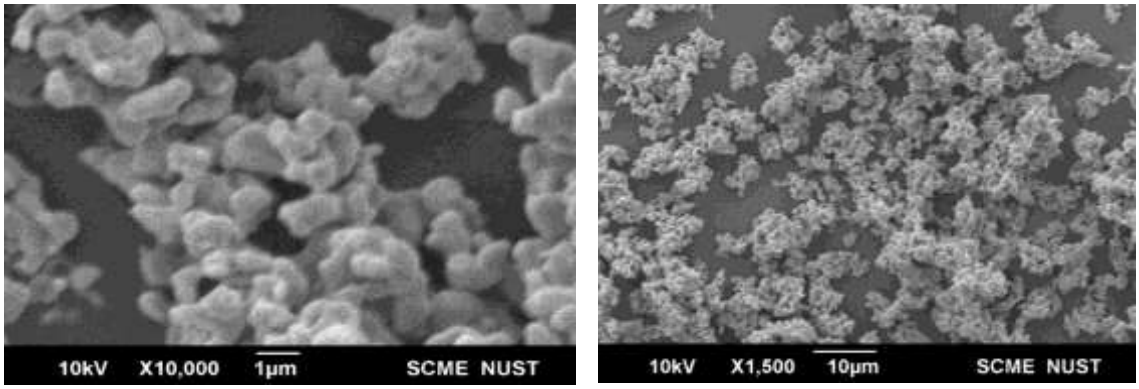

Figure 4. 8: *SEM images of cobalt particles*

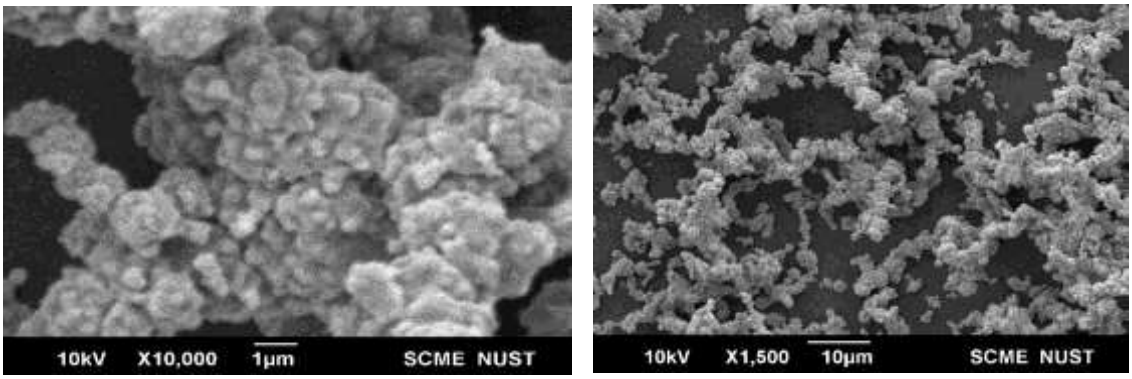

Figure 4. 9: *SEM images of nickel particles*

From Figure 4.6 and 4.7 we can see that there is no presence of other size particles in the powder material though the particles were of irregular shape but this is what we get from the supplier and also, we can see that at the same magnification nickel particles are larger than cobalt particles which conforms to the result of PSA test.

4.4.3 EDS (Energy Dispersive Spectroscopy)

The powders were tested under EDS machine to check the presence of any unwanted material. The results are shown in fig 4.8 and 4.9 and table 4.3 and 4.4

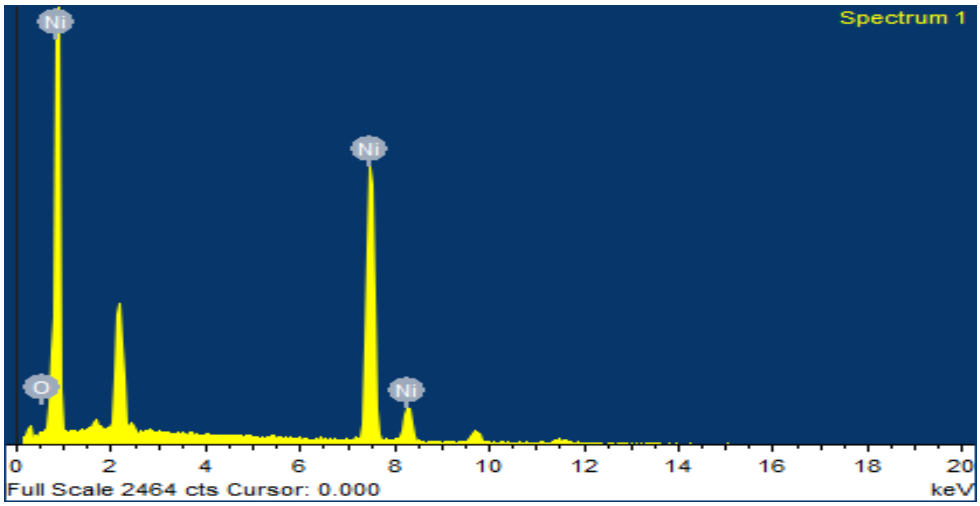

Figure 4. 10: *EDS spectrum for Nickel powder*

Table 4. 2: *EDS test result for Nickel*

Element	Weight (%)
O	0.49
Ni	99.51
Total	100

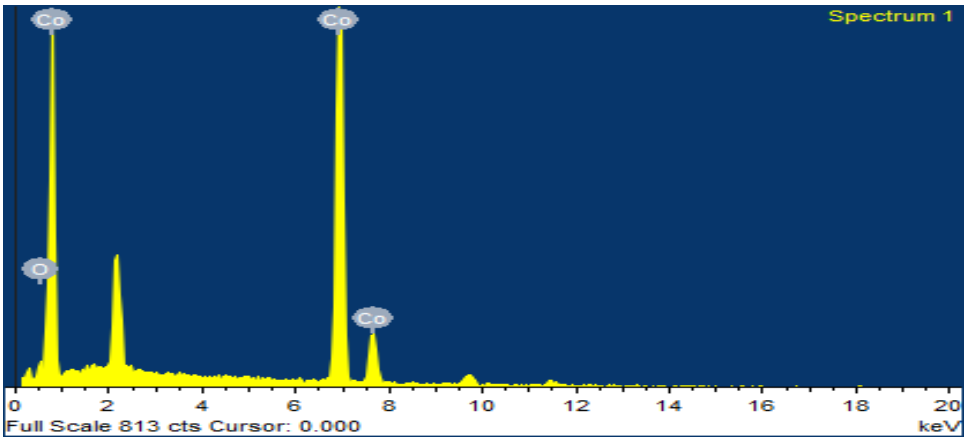

Figure 4. 11*: EDS spectrum of Cobalt powder*

Table 4. 3: *EDS test result for Cobalt*

Element	Weight (%)
O	3.57
Co	96.43
Total	100

From the results EDS test, we can see that both the Nickel and Cobalt powders don't contain any unwanted materials. There are traces of oxygen (3.57 % by weight) found along with cobalt particles but this small percentage doesn't have any major effect on our final test results.

4.5 Sample Preparation

To prepare the samples first the required volume of silicon rubber part A was mixed with the required volume of oil. Then the required amount of magnetic powder was added to the mixture followed by the hand mixing for five minutes. The mass was measured using the electronic balance. After five minutes of hand mixing the beaker was placed in the Ultrasonic cleaner bath Sonicator for one hour of sonication. Sonication was done for homogenous mixing of the mixture and to disperse the filler particles in the mixture to avoid agglomeration. Sonication was done in two batches each batch lasted for thirty minutes and each batch was followed by five minutes of hand mixing. After sonication Silicon rubber Part B was added and the liquid sample was then hand-mixed for ten minutes after which it was poured into the slots of a mold in layers along with slight tapping on the mold to prevent any bubble formation. Curing was done at room temperature for almost 24 hours and the samples were removed from the mold after they had cured properly.

Figure 4. 12: *Steps for casting of magnetorheological elastomers*

The Magnetorheological Elastomers that were casted were of size 23.62 x 12.5 mm and had a thickness of 14mm (figure 4.11). Three MRE samples were casted for a specific composition and of these three two were used for dynamic shear testing and one sample was used for sample micro-image analysis.

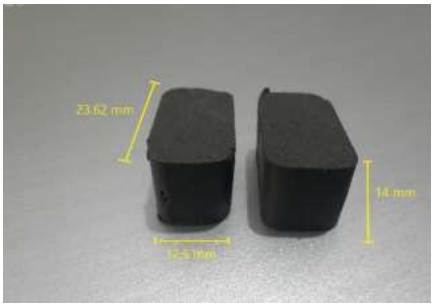

***Figure 4. 13**: MRE samples with Dimensions.*

After casting and curing of samples SEM test was performed on the samples to observe the dispersion of magnetic particles in the matrix and to check if there are any agglomerates present or not along with the voids. The SEM images for Nickel 5%,7.5% and 10% are shown in fig4.12, fig 4.13 and fig 4.14 respectively and SEM images for Cobalt 2.5% and 5% are shown in fig 4.15 and fig 4.16 respectively.

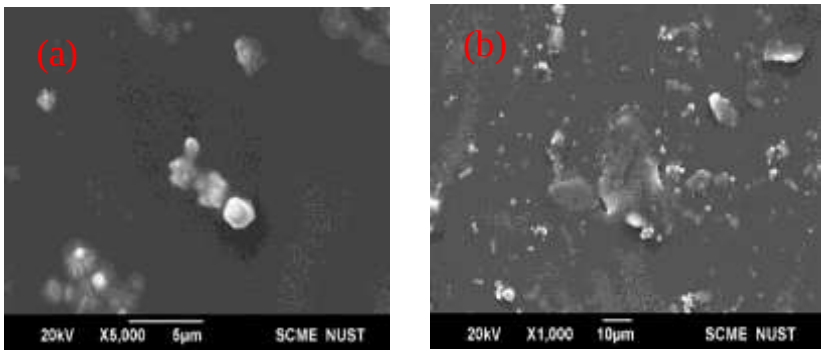

***Figure 4. 14:** (a) SEM image for Nickel 5% at X5,000 magnification. (b) SEM image for Nickel 5% at X1,000 magnification*

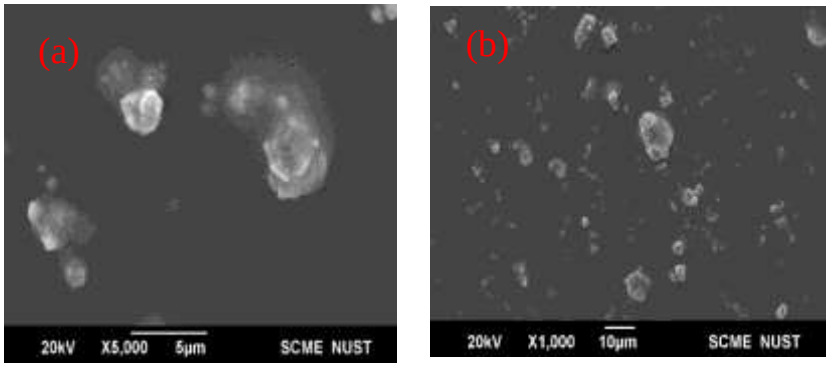

***Figure 4. 15:** (a) SEM image for Nickel 7.5% at 5000 magnifications. (b) SEM image for Nickel 7.5% at 1000 magnification*

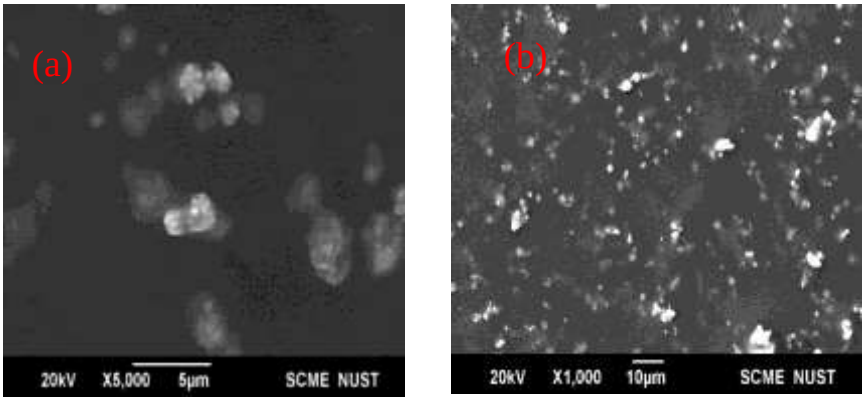

Figure 4. 16: *(a) SEM image for Nickel 10% at X5,000 magnification. (b) SEM image for Nickel 10% at X1,000 magnification*

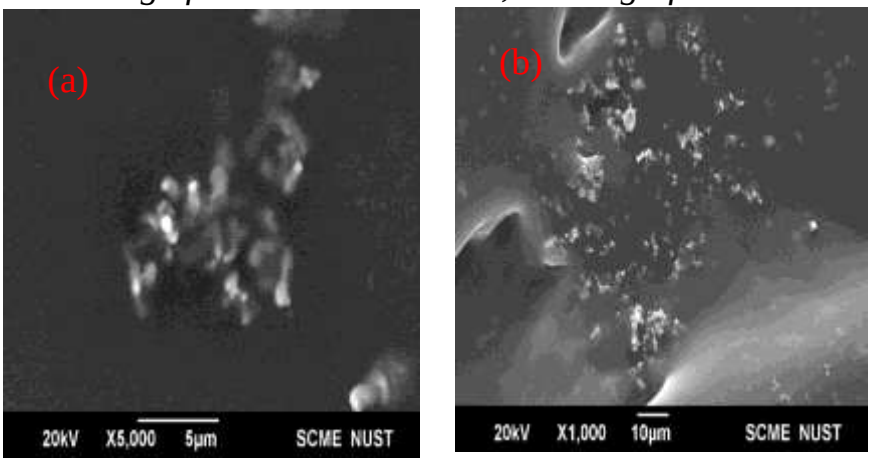

Figure 4. 17: *(a) SEM image for Cobalt 2.5% at X5,000 magnification. (b) SEM image for Cobalt 2.5% at X1,000 magnification*

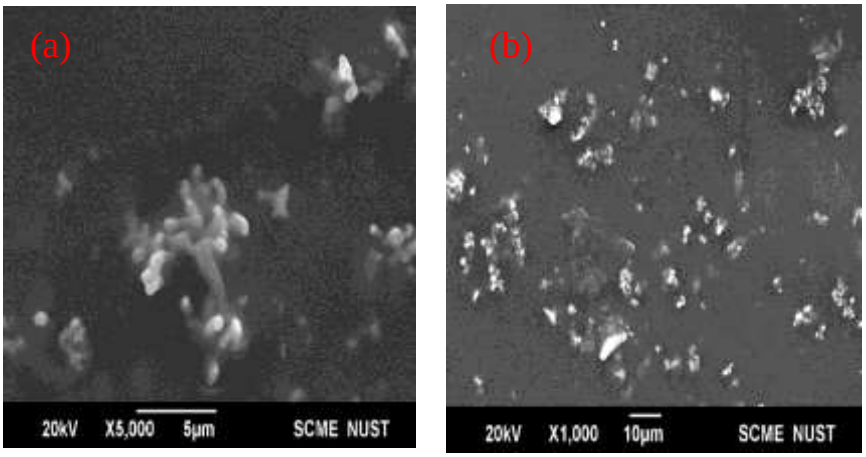

Figure 4. 18*: (a) SEM image for Cobalt 5% at 5000 magnification. (b) SEM image for Cobalt 5% at 1000 magnification.*

A total of seven compositions were prepared and for each composition, three samples were prepared. Two samples were used for testing and one sample was used for SEM imaging. SEM images for cobalt 7.5% and 10% were not included because these MRE samples didn't cure properly even after giving them a plenty of time. Also, we could not perform shear testing on these two samples. The compositions are summarized in Table 4.5

Table 4. 4: *Composition of MRE samples*

Sample Size (ISO – 1827): 23.62 mm x 12.5 mm x 14 mm					
S/No.	**Particle Name**	**No. of Samples for each Composition**	**Particle % by Volume of Sample**	**% of Elastomer**	**% of Silicon oil**
1.	Ni	3	5	85	10
2.	Ni	3	7.5	82.5	10
3.	Ni	3	10	80	10
4.	Co	3	2.5	87.5	10
5.	Co	3	5	85	10
6.	Co	3	7.5	82.5	10
7.	Co	3	10	80	10

CHAPTER 5: EXPERIMENTATION

5.1 Testing Parameters

To study and characterize dynamic behavior of MRE, it is important to consider different parameters based on previous research and testing machine limitations. Table 5.1 summaries the input parameters, their range and total number of test trials.

Table 5. 1: *Summary of Test Parameters*

Sr. no.	**Test Parameters**		**Range**
1	Filler Content	Nickel	5%, 7.5%, and 10% (by volume of MRE)
		Cobalt	2.5%, and 5% (by volume of MRE)
2	Frequency of vibration		0.5 Hz,1 Hz, 2Hz & 3 Hz
3	Amplitude of vibration		4.2 mm, 7mm & 9.8mm (30%,50%&70% strain)
4	Magnetic field		0T, 0.1 T, 0.2T, 0.3T & 0.4 T
Total No. of Samples: 5			
No. of Test on 1 sample: 60			
Total No. of Test cases: 300			

5.2 Testing Equipment

Dynamic testing was performed at National Textile University, Faisalabad, Pakistan using Zwick/ Roel Servo hydraulic testing machine (HC 25). Machine has the ability of performing cyclic loading with full control of changing frequency and amplitude at a wide range. It also has the computer system to record data along with cooling system.

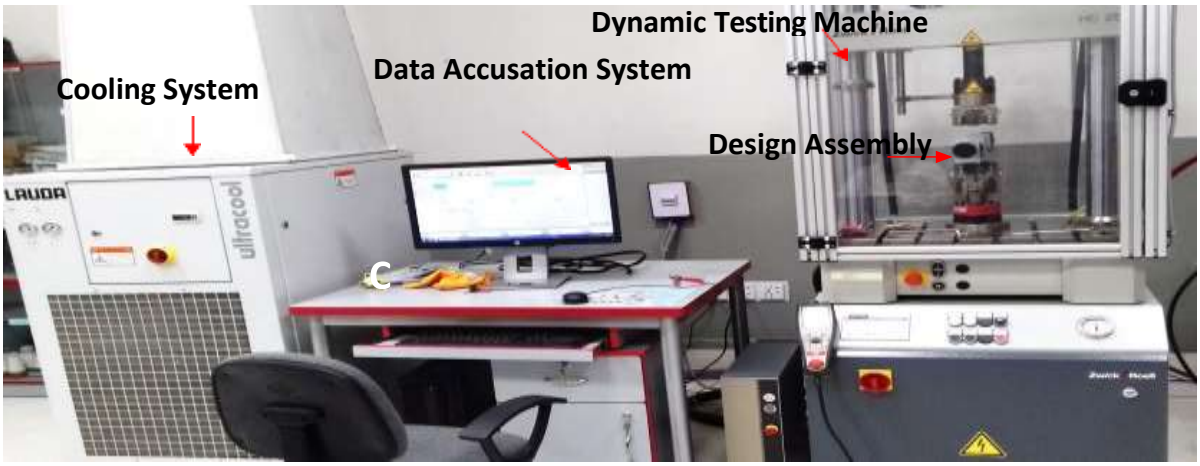

Figure 5. 1: *Zwick/ Roel Servo hydraulic testing machine with data accusation and cooling system5.3 Mechanism*

After carefully centring & gluing the two elastomers with aluminium strip and steel strips of design assembly. The machine was turned on along with data accusation system & its door was opened using a hydraulic valve. The design assembly was than fixed from bottom to the lower grip of machine and the upper aluminium strip which was sandwiched between MRE samples was fixed with the lower jaw of machine.

Testing was performed for the parameters mentioned in table 5.1. Input data was fed in computer with software linked with machine as shown in figure 5.2. Readings for 1st sample without magnetic field were taken by keeping the maximum distance between magnets and elastomers using adjustable knobs. For other magnetic field values, the knobs were adjusted by moving magnets closer to samples. The Magnetic flux values were measured using Gauss Meter. Samples were applied extra cycles of cycling loading to eliminate Mullin's effect so that hysteresis loops without any fluctuations can be obtained therefore, 12 cycles were considered for each test case. [40]

For the 1st test at 0 Tesla flux the frequency was kept constant and amplitude was varied, till whole amplitudes were covered (4.2, 7, 9.8 mm). Then process was repeated for 2nd frequency and so on. After completing all frequencies (0.5, 1, 2, 3) the magnetic flux value was changed. The process was repeated for all the values of magnetic flux (0, 0.1, 0.2, 0.3, 0.4Tesla), resulting into 60 tests on one sample of MRE. After completing test on 1st sample the whole assembly was removed from machine, 2nd MRE samples (S2) was attached with assembly after properly scrubbing off the superglue from the surface of strips. The same testing sequence was repeated for all samples yielding 300 test cases in total.

Figure 5. 2: *Computer system linked with Dynamic testing machine to enter input data and to extract results.*

5.4 Extraction of results

The data for testing was saved in computer after each test in separate folders with different names. After completion of all 300 tests, the results were extracted from the computer in the form of time vs. displacement, time vs. force, force vs. displacement, Dynamic stiffness. Damping values for each individual test.

5.5 Post processing of results

The extracted data from machine software was processed in MATLAB (R2018b) Software to remove noise or any bias from the test data by using sgolayfilt filter which can be seen in Fig 5.3. Finally, graphs were plotted, and stiffness values were determined from graphs.

In general elastomers are categorized by their stiffness parameters, due to simplicity of its measurements and its relationship with other mechanical constants such as, shear and elastic modulus. The effective stiffness is calculated according to author Li et al [38].

Effective stiffness= Kef = (Max Force−Min Force) / (Max Displacement−Min Displacement)

Where:

Max force= It's the maximum positive value of force on force-displacement loops.

Min force= It’s the maximum negative value of force on force-displacement loops.

Max Displacement= Maximum displacement value corresponding to maximum force.

Min Displacement= Maximum displacement value corresponding to maximum force.

```
Disp=T.data(:,7);
Force=T.data(:,10);
ForceFil=sgolayfilt(Force,1,61);
```

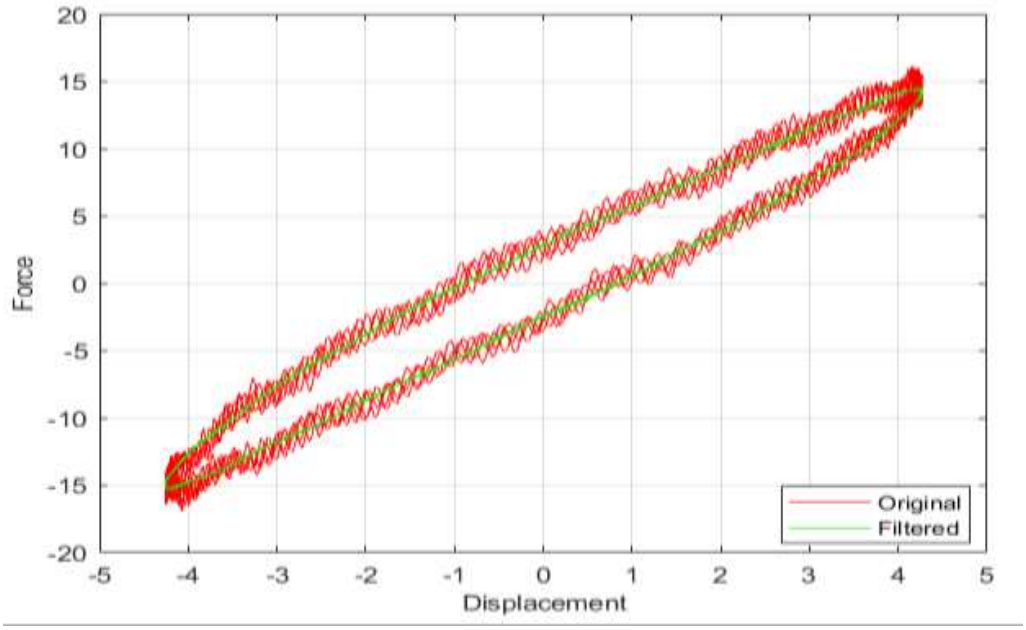

Figure 5. 3: *Comparison of Filtered and Unfiltered Data*

CHAPTER 6: RESULTS AND DISCUSSION

For observing the MR effect of MREs filled with nickel and cobalt magnetic particles, dynamic shear test was performed, and force-displacement data was obtained for 12 cycles. Out of 12 cycles 8 cycles are deducted, 4 cycles from start and 4 cycles from end and middle cycles are used.

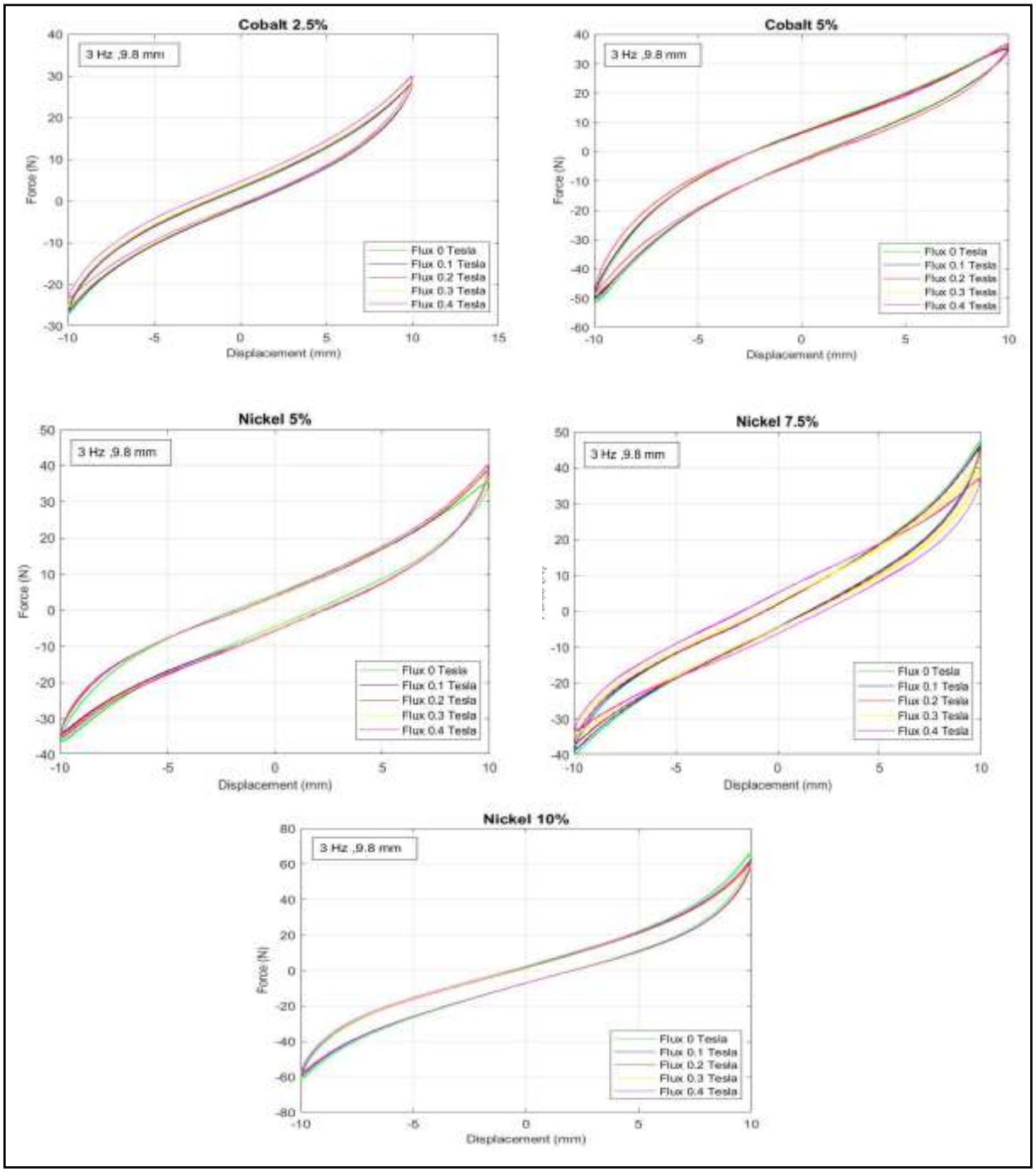

Figure 6. 1*: Hysteresis loops of all 5 samples for highest values of frequency & amplitude*

As the behavior of MREs cannot be easily discuss from the results obtained from Dynamic Shear testing, therefore filters in MATLAB were used to make them easily understandable. The force-displacement plots are basically hysteresis loops with loading and unloading curves. The hysteresis loops of all samples at highest frequency and amplitude are shown in figure 6.1.

6.1 General Observation

In Fig 6.1 the hysteresis loops of cobalt 2.5% shows increase in steepness except at 9.8 mm amplitude where it shows decrease in steepness while nickel 5% shows the increase in steepness with increase in the magnetic flux, firstly the steepness decreases at 0.1 Tesla then an increase is observed at 0.2 Tesla then again decrease at 0.3 Tesla afterwards shows increase up to 0.4 Tesla. Nickel 7.5% and Nickel 10% shows decrease in steepness of loops with change in magnetic flux at constant frequency and amplitude while for Cobalt 5% a decrease in steepness is observed up to 0.2 Tesla then slight increase at 0.3 Tesla then again decrease at 0.4 Tesla which is more elaborated in Fig 6.9. The stiffness of the force-displacement loops is calculated according to Li.et.al [38].

MR effect is basically the increase in stiffness with increase in magnetic flux i.e., from 0 Tesla to 0.4 Tesla [1].By closely observe the hysteresis graphs as elaborated in Fig 6.1 it is noted that increase in stiffness increase (%) is observed with increase in frequency from 0.5 Hz to 3 Hz while decrease in stiffness increase (%) is observed with increase in amplitude except nickel 5% at all frequencies and at 0.5 Hz for other samples where stiffness increase (%) first decreases then increases at 9.8 mm. Moreover, the area of loops shows the damping effect of MREs [38]. By observing the hysteresis graphs, it is noted that the damping is increasing with increase in the filler content (%).

Figure 6.2 shows the max effective stiffness for Nickel and Cobalt MREs. Among nickel samples, nickel 10% shows max stiffness of 6.39 N/mm which is 43% higher than nickel 7.5% and 69% higher than nickel 5%. For cobalt samples, cobalt 5% shows max effective stiffness which is 35% higher than cobalt 2.5%. It can be observed that max effective stiffness increases with increase in filler content (%). Among nickel and cobalt samples cobalt shows more stiffness than nickel sample which is 35% higher.

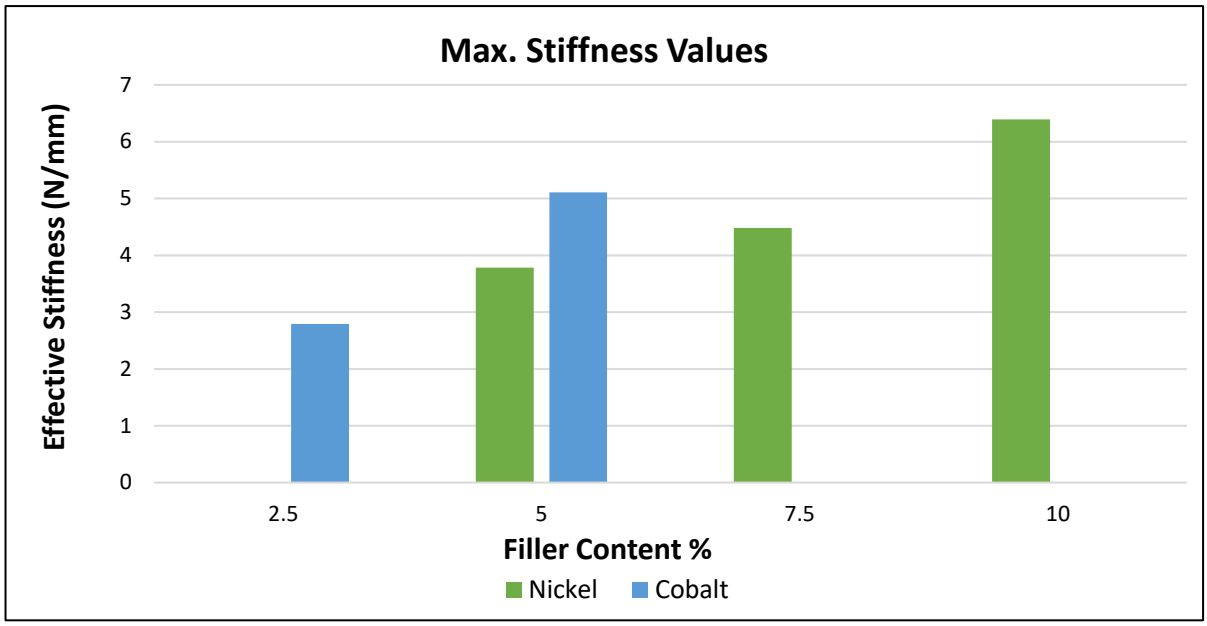

Figure 6. 2: *Plot to compare Max Stiffness values of all samples*

6.2 Effect of Changing Amplitude

Figure 6.3 shows the hysteresis plot of force-displacement with changing amplitude. Nickel 5% and Cobalt 5% are considered to represent the MREs. The behavior of MRE with change in amplitude is easily distinguishable. It shows that with increase in amplitude the force increases which shows the amplitude dependent nature of MREs. By observing the hysteresis graphs under constant flux, frequency and changing amplitude the steepness of force-displacement plots is decreasing with increasing amplitude along with the shape change

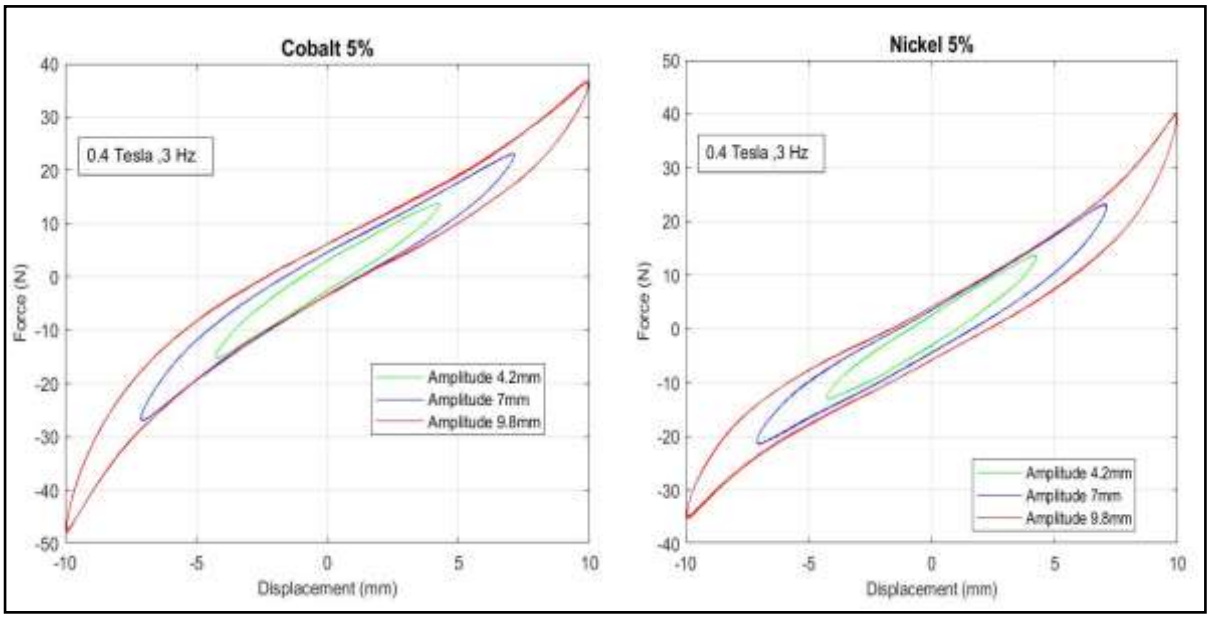

Figure 6. 3*: Hysteresis plots of MREs with varying amplitudes under 0.4 T flux density at 3 Hz frequency for (a) Cobalt 5% (b) Nickel 5%"*

showing strain stiffening at high amplitude. Strain stiffening is the phenomenon of limiting the extensibility of polymer chains which is more pronounce in natural rubber. For MR elastomers the strain stiffening (non-linearity) is more pronounced at higher flux values indicating more limiting in extensibility of polymer chains [1]. More strain stiffening observed at 0.4 Tesla than 0 Tesla. Figure 6.3 shows the increase in area of hysteresis loops with increase in amplitude which depicts MREs have more damping effect at high amplitudes. Through visual observation cobalt 5% shows more damping effect than nickel 5%.

Figure 6.4 shows the change in effective stiffness with change in amplitude under different frequencies. It can be seen that highest stiffness is prominent in Nickel 5%. In cobalt 2.5% the increase in stiffness with increase in amplitude is observed while for nickel 5% trend is not the same. In Nickel 5% at first decrease in stiffness at 7 mm amplitude then increase is observed at 9.8mm. Increase in stiffness is observed with increase in frequency for both samples while more increase in stiffness is observed with change in frequency in nickel 5% as compared to cobalt 2.5%."According to literature for MREs with micro particles, stiffness decreases with increase in strain even for larger strains stiffness decreases with increase in strains [39,40,41].But in present research for cobalt stiffness is constant up to 50% strain (i.e., 7 mm) then increases up to 70% strain (i.e., 9.8 mm) while for nickel at first decrease is observed up to 50% strain (i.e., 7 mm) then increases (i.e., 9.8 mm).

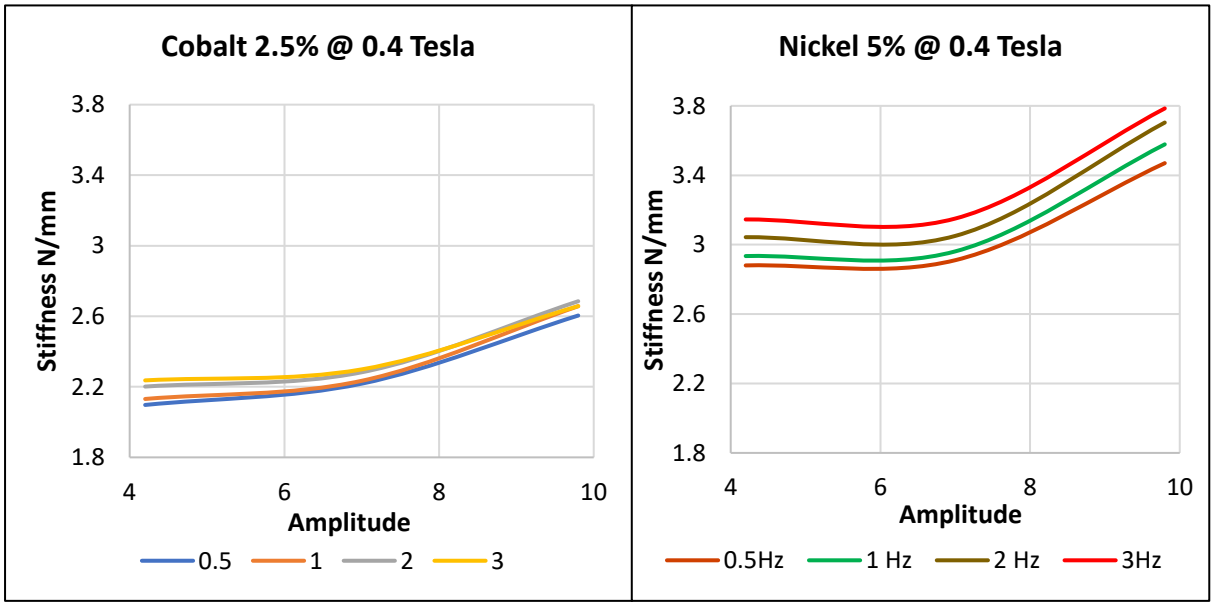

Figure 6. 4: *Effective Stiffness versus changing Amplitude under different Frequencies for (a) Cobalt 2.5% (b) Nickel 5%"*

6.3 Effect of Changing Frequency

Figure 6.3 shows the hysteresis plot of force-displacement with changing frequency under constant flux and amplitude. With increase in frequency the steepness of hysteresis loops is increasing indicating increase in stiffness. Change in shape of loops is very less with increase in frequency as compared to change in amplitude. The area of loop is also increasing with increase in frequency indicating more damping effect at high frequencies. Same trend is observed for flux greater than and equal to 0.2 T while for less than 0.2 T decrease in stiffness is observed with increase in frequency.

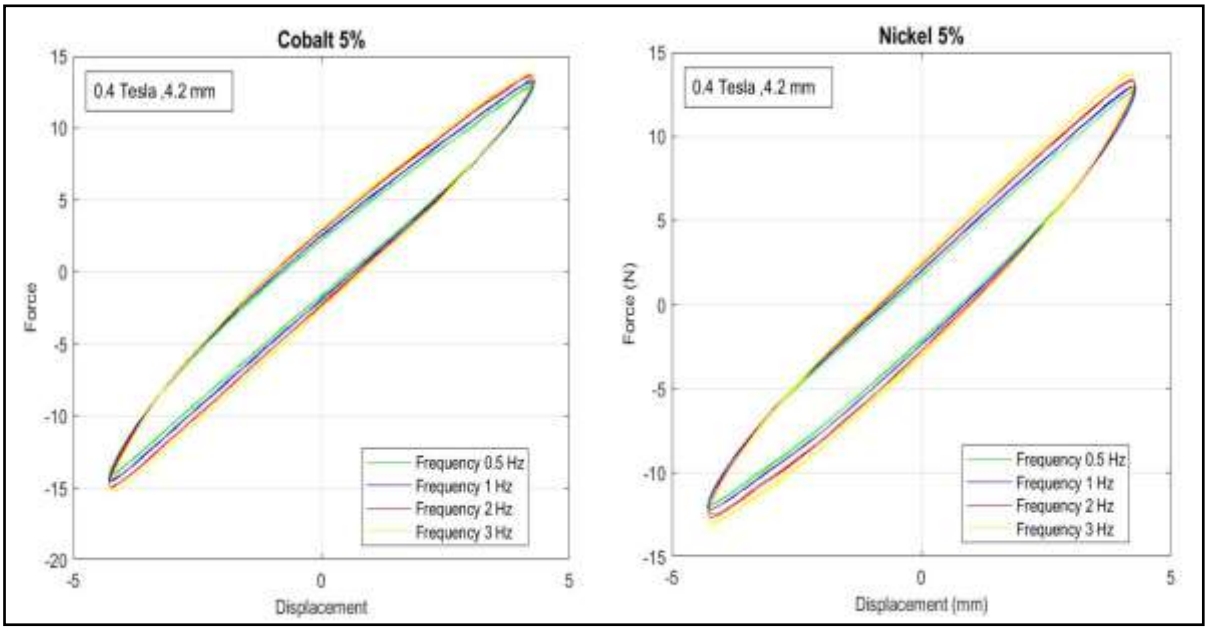

Figure 6. 5: *Hysteresis plots of MREs with varying Frequency under 0.4 T Flux density at 4.2 mm Amplitude for (a) Cobalt 5% (b) Nickel 5%*

Figure 6.6 shows the change in effective stiffness with change in frequency under different amplitudes at constant flux. It can be seen that max effective stiffness is prominent in Nickel 5%. With increase in frequency decrease in stiffness is observed up to 1 Hz after that a constant trend is following which shows that effective stiffness depends slightly on frequency. With increase in amplitude effective stiffness increasing for both samples.

Figure 6.7 shows the change in effective stiffness with change in frequency at 0.4 Tesla. It can be seen that the increase in stiffness with increase in frequency is observed while for 0 Tesla decrease in stiffness was occurring. The increase trend is same for 0.2-0.4 Tesla while for 0-0.1 Tesla decrease trend is followed. As in case of Nickel 5% the stiffness increase in 7 mm is

not following the trend that may be due to instrument error or loose of bond between MRE and Aluminum Strip.

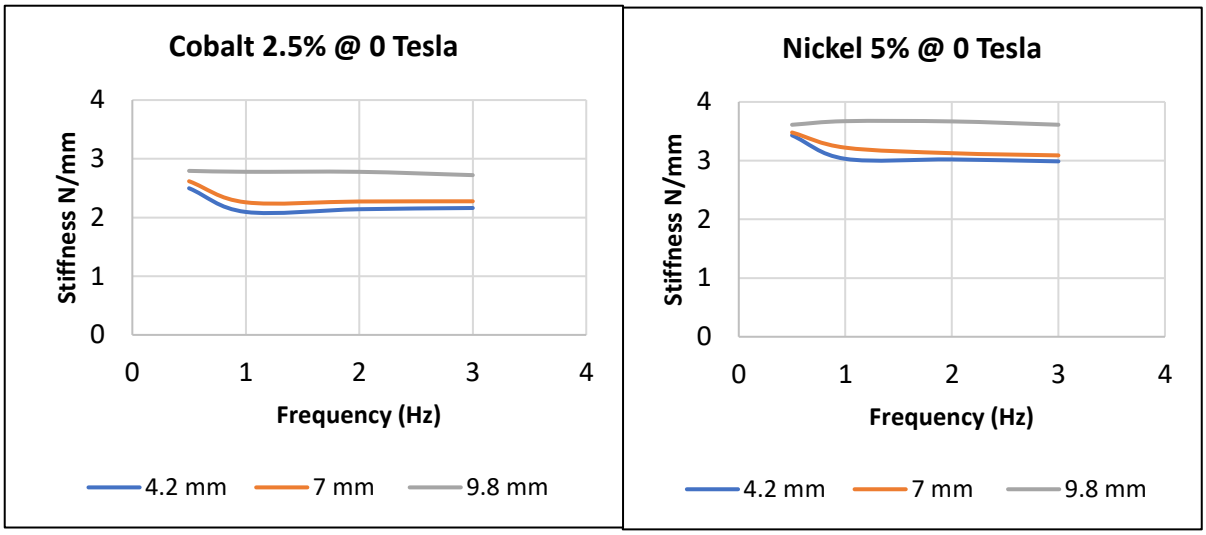

Figure 6. 6: *Effective Stiffness versus changing Frequency under different Amplitude at 0 Tesla for (a) Cobalt 2.5% (b) Nickel 5%*

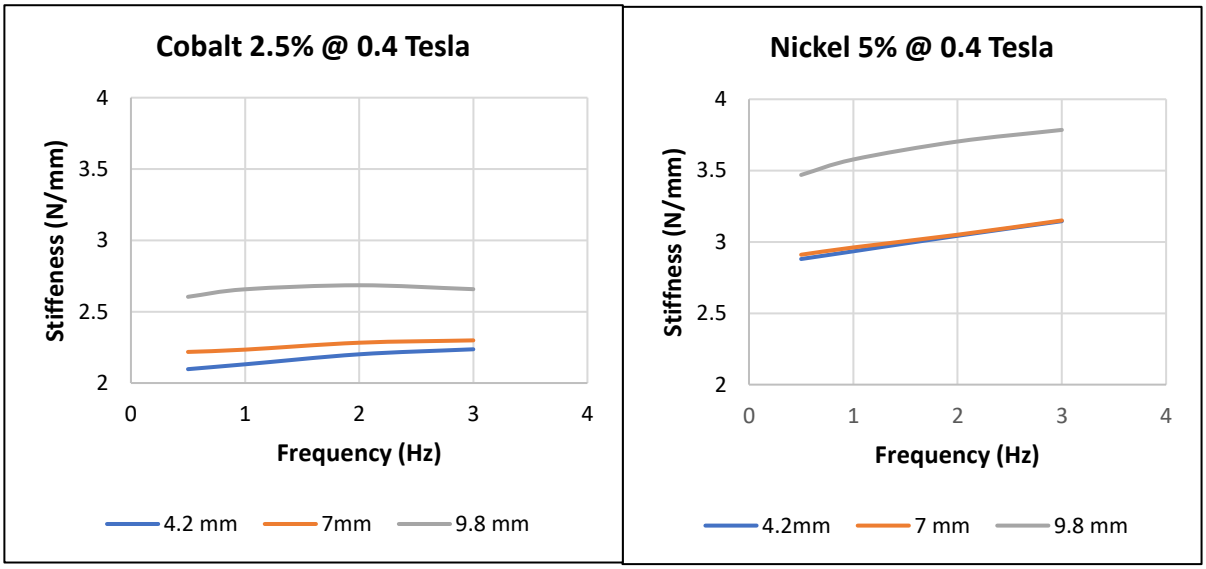

Figure 6. 7: *Effective Stiffness versus changing Frequency under different Amplitude at 0.4 Tesla for (a) Cobalt 2.5% (b) Nickel 5%*

6.4 Effect of Changing Magnetic Flux

Figure 6.8 shows the change in stiffness with change in magnetic flux under different amplitudes. It can be seen that with increase in magnetic flux the stiffness is increasing for both samples except for cobalt 2.5% at 9.8mm. With increase in amplitude the increase in stiffness can also be observed while for other sample the decrease in stiffness is observed with increase in flux. The change of stiffness with change in flux shows the influence of magnetic field on the magnetic filler particles.

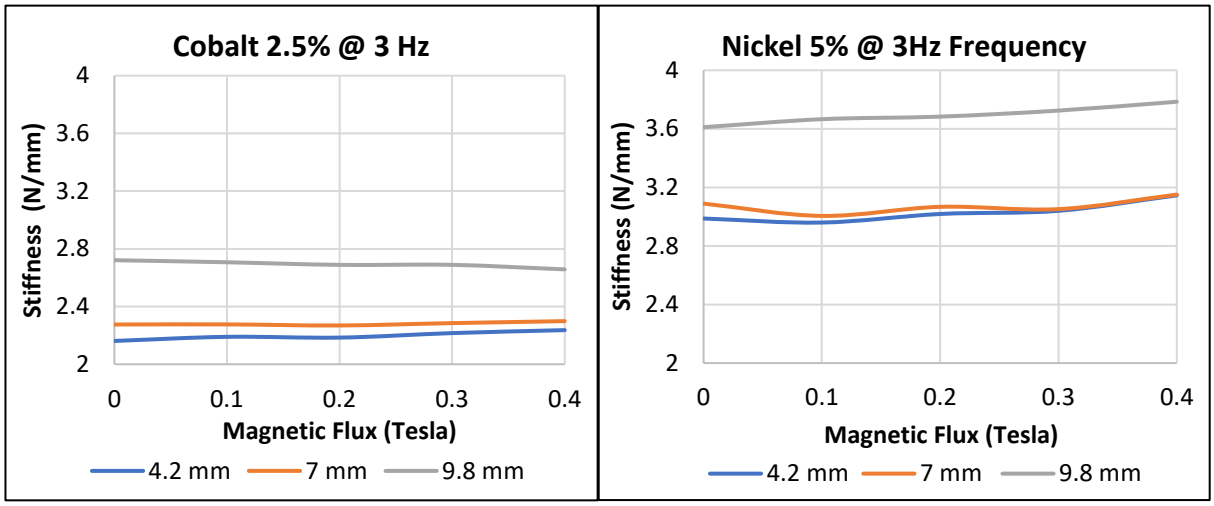

***Figure 6. 8**: Effective Stiffness versus changing Flux under different Amplitude at 3 Hz for (a) Cobalt 2.5% (b) Nickel 5%*

6.5 Magnetorheological Effect:

Figure 6.9 shows that with increase in amplitude the increase in stiffness decreases linearly for cobalt 2.5% while for nickel 5% stiffness first decreases up to 50% strain (7 mm) then increases. For cobalt 2.5% at 0.5 Hz increase in stiffness remain constant up to 50% strain then increases. Same trends are observed in [5] for nano and hybrid samples.

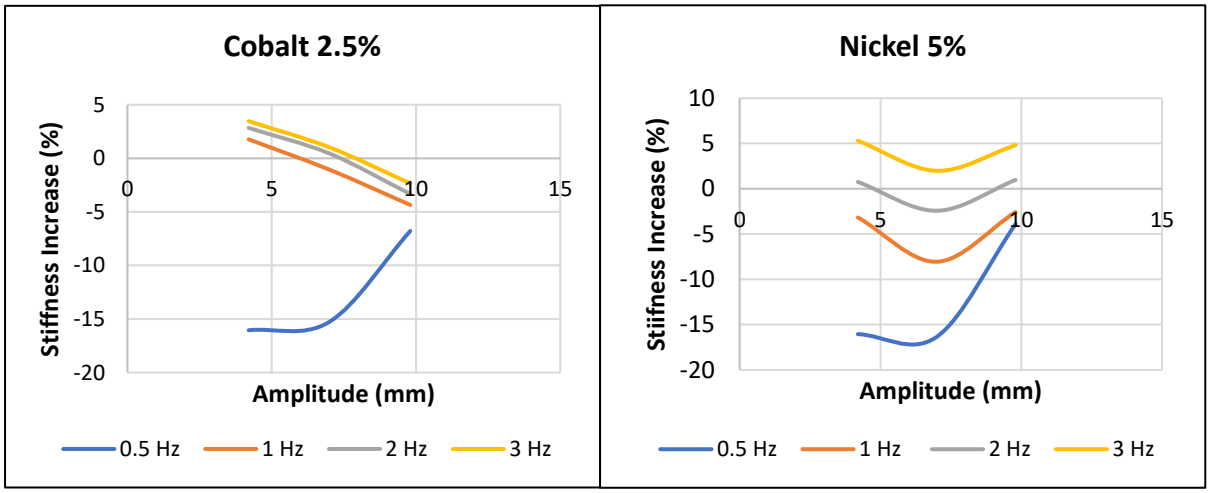

***Figure 6. 9:** Effect of Magneto-rheology on Effective stiffness increase due to change in amplitude for (a) Cobalt 2.5% (b) Nickel 5%"*

Decrease of MR effect with increase in strain is attributed to Payne effect, in which at high strains rubber molecules start to slide which causes increase in inter-molecular distance due to which distance between ferromagnetic particles increases and results in reduction of MR effect [42,43,44]. Fig 6.9 shows that with increase in frequency increase in stiffness increases while according to the literature for micro-particles the increase in stiffness decreases or remain

constant with increase in frequency and according to [5] for nano and hybrid samples increase in stiffness increases with increase in frequency. For sample with cobalt particles, increase in stiffness first increases up to 1 Hz then remain constant.

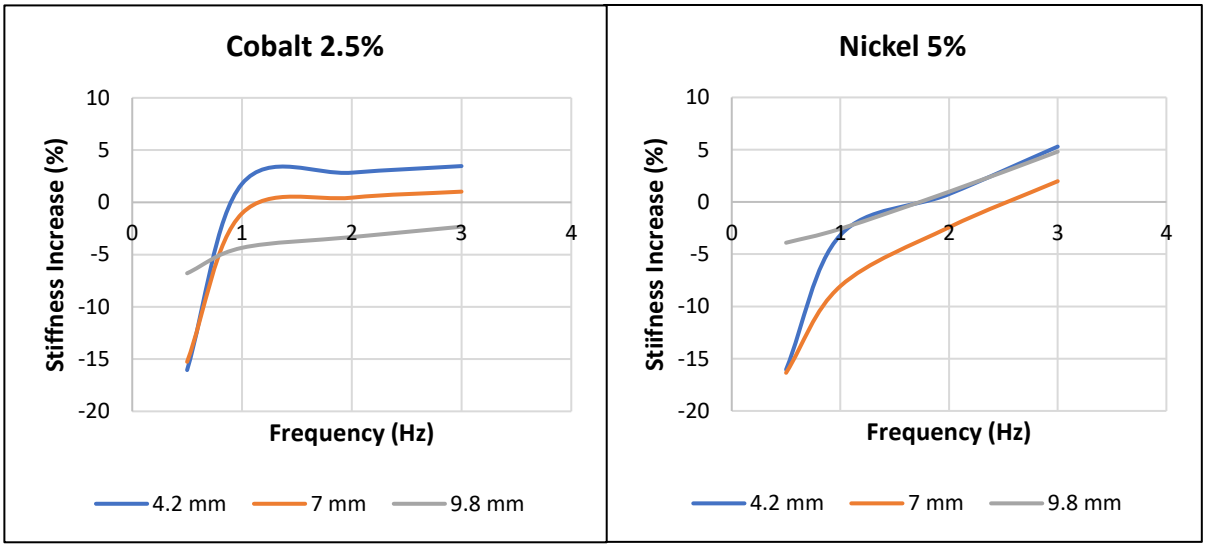

Figure 6. 10: *Effect of Magneto-rheology on Effective stiffness increase due to change in amplitude for (a) Cobalt 2.5% (b) Nickel 5%"*

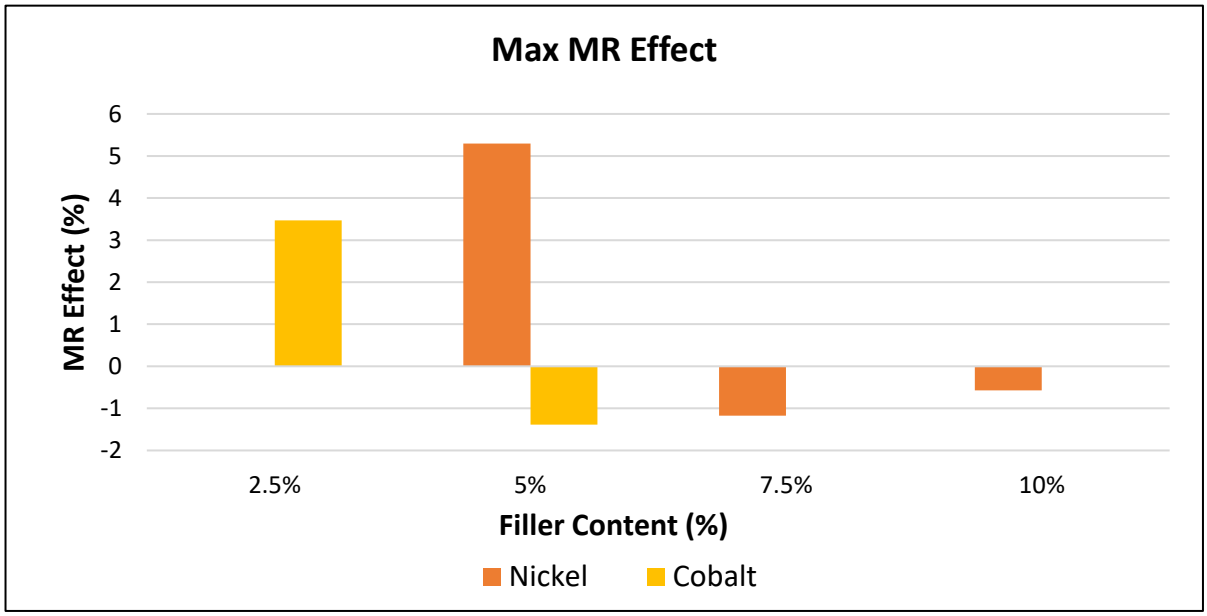

Figure 6. 11*: Maximum values of MR effect for all sample*

For more clear understanding, MR effect and effective stiffness with minimum and max flux of nickel samples at highest frequency and different amplitudes are represented in Table 6.1. It shows that nickel has max stiffness increase of 5.3% for 5% content while for 7.5 and 10% max stiffness increase are -1.2% and -0.6% respectively. It can be observed in Fig 6.1 hysteresis loops that for nickel samples with 7.5% and 10% filler content force at 0 flux is more than with

Table 6. 1: *Stiffness Increase (%) Calculation for Nickel samples at highest frequency for all three amplitudes (a) 4.2 mm (b) 7mm (c) 9.8 mm*

		3 Hz Frequency, 4.2 mm Amplitude		
Sample	**% Content of Filler**	**0 Tesla Stiffness**	**0.4 Tesla Stiffness**	**% Increase in Stiffness**
Nickel	**5**	2.987325	3.145532	5.295952
	7.5	3.476281	3.435409	-1.17574
	10	4.5247	4.4987	-0.57462
		3 Hz Frequency, 7 mm Amplitude		
	5	3.089284	3.150576	1.984013
	7.5	3.573144	3.201167	-10.4104
	10	4.7063	4.6185	-1.86558
		3 Hz Frequency, 9.8 mm Amplitude		
	5	3.611286	3.785164	4.814841
	7.5	4.376534	3.539233	-19.1316
	10	6.0557	5.8058	-4.12669

flux. For nickel 7.5 and 10 % content samples, difference of higher to lower flux results into negative MR effect. Out of nickel samples, samples with 5% filler content shows more better results for MR effect as compared to 7.5% and 10% samples.

Figure 6.10 shows max MR effect of all samples. It is clear from figure that max MR effect shown by cobalt decrease with increase in filler content while for nickel MR effect first

decrease up to 7.5% then slightly increases up to 10%. Both filler materials show better MR effect at low filler content which suggests the use of filler content at low percentages. From Figure 6.2 and 6.10 it can be seen that nickel has minimum stiffness and highest MR at 5% while for nickel 10% has more stiffness than nickel 7.5% and nickel 10% is showing more MR effect which suggest to do research on nickel with high filler content. In case of Cobalt with increase in stiffness decrease in MR effect is observed. Out of nickel and cobalt, it is clear that nickel has 4.8% more effect than cobalt at 5%.

CHAPTER 7: CONCLUSIONS & RECOMMENDATIONS

7.1 CONCLUSION

The research focus was to understand and characterize the behavior of MRE's compose of different type of filler contents under different loading (frequency, amplitude of vibration) and magnetic flux conditions. Following conclusions can be obtained from the results.

- For nickel and cobalt based MREs, change in effective stiffness with change in frequency is in line with the previous researches and less as compared to change in amplitude which shows amplitude dependent nature of MREs.
- More increase in stiffness is observed at 70% strain as compared to 50% strain which is a new finding and need further research.
- For nickel and cobalt based MREs, MR effect increases with increase in frequency which is a new observation with microparticles and requires further research.
- For cobalt based MREs, MR effect with change in amplitude is in line with the literature. But for nickel based MREs, increase in MR effect is observed at 70% strain as compared to 50% strain which is a new observation and need more research.
- For nickel and cobalt based MREs higher MR effect was observed for lower filler percentages which is opposite to the trend observed in literature for carbonyl iron based MREs containing microparticles.
- Higher MR effect was observed in case of nickel based MREs compared to cobalt based MREs which validates the previous researches that with increase in initial stiffness reduction in MR effect will occur.
- MR effect due to use of carbonyl iron in previous studies observed more than as compared to nickel and cobalt based MREs this validates that for MREs with high initial stiffness gives less MR effect.

7.2 RECOMMENDATIONS

- As this research was limited to only one size for both fillers while there is a need of detailed research on the effect of size of filler particles on the MR effect.

- In view of this research, decrease in MR effect with increase in filler content is not according to literature which needs further research which can be done by decreasing initial stiffness.
- As this research was limited to only filler content less than 10% due to not curing of samples at high percentage. Research is required at higher filler content by making samples curable using some admixtures.

REFERENCES

1. Li, Y.; Li, J.; Tian, T.; Li, W. A Highly Adjustable Magnetorheological Elastomer Base Isolator for Applications of Real-Time Adaptive Control. Smart Materials and Structures 2013, 22, 095020.[CrossRef]
2. Anna Boczkowska; Stefan Awietjan. Microstructure and Properties of Magnetorheological Elastomer. Advanced Elastomers – Technology. 2012.[CrossRef]
3. State of the art of control schemes for smart systems featuring magneto-rheological materials. Seung-Bok Choi, Weihua Li, Miao Yu, Haiping Du, Jie Fu and Phu Xuan Do. Smart Materials, 2016. [CrossRef]
4. A model of the behavior of magnetorheological materials. Mark R Jolly, J David Carlson and Beth C Muñoz. Smart Materials, 1996. [CrossRef]
5. S.U.Khayam, M.Usman. Development and characterization of a novel hybrid magnetorheological elastomer incorporating micro and nano size iron fillers. Materials and Design, 2020. [CrossRef]
6. Davis, L. Model of Magnetorheological Elastomers. *Journal of Applied Physics* 1999. [CrossRef]
7. Jabob Rabinow, The magnetic fluid clutch, Electrical Engineering, 1948. [CrossRef]
8. Jin, Q.; Xu, Y.; Di, Y.; Fan, H. Influence of The Particle Size on The Rheology Of Magnetorheological Elastomer. Materials Science Forum 2014, 809-810, 757-763. [CrossRef]
9. NA Yunus, SA Mazlan. Thermal Stability and Rheological Properties of Epoxidized Natural Rubber-Based Magnetorheological Elastomer. International Journal of Molecular sciences. 2019. [CrossRef]
10. H J Song, N M Wereley. Field dependent response of magnetorheological elastomers utilizing spherical Fe particles versus Fe nanowires. Journal of Physics. 2009. [CrossRef]
11. RA Landa, PS Antonel. Magnetic and elastic anisotropy in magnetorheological elastomers using nickel-based nanoparticles and nanochains. Journal of Applied Physics, 2013. [CrossRef]
12. Koo, Jeong-Hoi, Alexander Dawson, and Hyung-Jo Jung. "Characterization of actuation properties of magnetorheological elastomers with embedded hard magnetic particles." Journal of Intelligent Material Systems and Structures 23, no. 9 (2012): 1049-1054. [CrossRef]
13. Sun, T. L., X. L. Gong, W. Q. Jiang, J. F. Li, Z. B. Xu, and W. H. Li. "Study on the damping properties of magnetorheological elastomers based on cis-polybutadiene rubber." Polymer Testing 27, no. 4 (2008): 520-526. [CrossRef]
14. Lokander, Mattias, and Bengt Stenberg. "Performance of isotropic magnetorheological rubber materials." Polymer Testing 22, no. 3 (2003): 245-251. [CrossRef]
15. Wei, Bing, Xinglong Gong, and Wanquan Jiang. "Influence of polyurethane properties on mechanical performances of magnetorheological elastomers." Journal of applied polymer science 116, no. 2 (2010): 771-778. [CrossRef]
16. Kukla, Mateusz, Łukasz Warguła, Krzysztof Talaśka, and Dominik Wojtkowiak. "Magnetorheological elastomer stress relaxation behavior during compression: experiment and modelling." Materials 13, no. 21 (2020): 4795. [CrossRef]
17. Miedzinska, Danuta, Anna Boczkowska, and Konrad Zubko. "Numerical verification of three-point bending experiment of magnetorheological elastomer (MRE) in magnetic field." In Journal of Physics: Conference Series, vol. 240, no. 1, p. 012158. IOP Publishing, 2010. [CrossRef]

18. Gorman, Dave. "The Evaluation and Implementation of Magnetic Fields suitable for Biaxial Cyclic Testing of Magnetorheological Elastomers." (2017). [CrossRef]
19. Bastola, Anil K., Milan Paudel, and Lin Li. "Magnetic circuit analysis to obtain the magnetic permeability of magnetorheological elastomers." Journal of Intelligent Material Systems and Structures 29, no. 14 (2018): 2946-2953. [CrossRef]
20. Chavez, Jhohan, Marek Ziolkowski, Philipp Schorr, Lothar Spieß, Valter Böhm, and Klaus Zimmermann. "A method to approach constant isotropic permeabilities and demagnetization factors of magneto-rheological elastomers." Journal of Magnetism and Magnetic Materials 527 (2021): 167742. [CrossRef]
21. Lerner, A. Albanese, and K. A. Cunefare. "Performance of MRE-based vibration absorbers." Journal of Intelligent Material Systems and Structures 19, no. 5 (2008): 551-563. [CrossRef]
22. Drozdov, Aleksey D., and Al Dorfmann. "The stress–strain response and ultimate strength of filled elastomers." Computational materials science 21, no. 3 (2001): 395-417. [CrossRef]
23. Arslan Hafeez, Muhammad, Muhammad Usman, Malik Adeel Umer, and Asad Hanif. "Recent Progress in Isotropic Magnetorheological Elastomers and Their Properties: A Review." Polymers 12, no. 12 (2020): 3023. [CrossRef]
24. Von Lockette, Paris R., Jennifer Kadlowec, and Jeong-Hoi Koo. "Particle mixtures in magnetorheological elastomers (MREs)." In Smart Structures and Materials 2006: Active Materials: Behavior and Mechanics, vol. 6170, p. 61700T. International Society for Optics and Photonics, 2006. [CrossRef]
25. Tian, Tongfei, and Masami Nakano. "Fabrication and characterisation of anisotropic magnetorheological elastomer with 45 iron particle alignment at various silicone oil concentrations." Journal of Intelligent Material Systems and Structures 29, no. 2 (2018): 151-159. [CrossRef]
26. Khairi, M. H. A., Siti Aishah Abdul Aziz, N. M. Hapipi, Saiful Amri Mazlan, Nur Azmah Nordin, and N. I. N. Ismail. "Enhancement of Isotropic Magnetorheological Elastomer Properties by Silicone Oil." In Proceedings of the 6th International Conference and Exhibition on Sustainable Energy and Advanced Materials, pp. 285-292. Springer, Singapore, 2020. [CrossRef]
27. Jung, Hyung-Jo, Sung-Jin Lee, Dong-Doo Jang, In-Ho Kim, Jeong-Hoi Koo, and Fazeel Khan. "Dynamic characterization of magneto-rheological elastomers in shear mode." IEEE transactions on magnetics 45, no. 10 (2009): 3930-3933. [CrossRef]
28. Usman, Muhammad, Dong-Doo Jang, In-Ho Kim, Hyung-Jo Jung, and Jeong-Hoi Koo. "Dynamic testing and modeling of magneto-rheological elastomers." In Smart Materials, Adaptive Structures and Intelligent Systems, vol. 48968, pp. 495-500. 2009. [CrossRef]
29. Popp, Kristin M., Matthias Kröger, Wei hua Li, Xian Zhou Zhang, and Prabuono B. Kosasih. "MRE properties under shear and squeeze modes and applications." Journal of Intelligent Material Systems and Structures 21, no. 15 (2010): 1471-1477. [CrossRef]
30. Poojary, Umanath R., and K. V. Gangadharan. "Integer and fractional order-based viscoelastic constitutive modeling to predict the frequency and magnetic field-induced properties of magnetorheological elastomer." Journal of Vibration and Acoustics 140, no. 4 (2018). [CrossRef]
31. Li, Yancheng, Jianchun Li, Tongfei Tian, and Weihua Li. "A highly adjustable magnetorheological elastomer base isolator for applications of real-time adaptive control." Smart Materials and Structures 22, no. 9 (2013): 095020. [CrossRef]

32. Jin, Qian, Yong Gang Xu, Yang Di, and Hao Fan. "Influence of the particle size on the rheology of magnetorheological elastomer." In Materials Science Forum, vol. 809, pp. 757-763. Trans Tech Publications Ltd, 2015. [CrossRef]
33. Winger, J., M. Schümann, A. Kupka, and S. Odenbach. "Influence of the particle size on the magnetorheological effect of magnetorheological elastomers." Journal of Magnetism and Magnetic Materials 481 (2019): 176-182. [CrossRef]
34. Sarkar, Chiranjit, and Harish Hirani. "Development of a magnetorheological brake with a slotted disc." Proceedings of the Institution of Mechanical Engineers, Part D: Journal of Automobile Engineering 229, no. 14 (2015): 1907-1924. [CrossRef]
35. Demchuk, S. A., and V. A. Kuz'min. "Viscoelastic properties of magnetorheological elastomers in the regime of dynamic deformation." Journal of Engineering Physics and Thermophysics 75, no. 2 (2002): 396-400. [CrossRef]
36. Poojary, Umanath R., Sriharsha Hegde, and K. V. Gangadharan. "Experimental investigation on the effect of carbon nanotube additive on the field-induced viscoelastic properties of magnetorheological elastomer." Journal of materials science 53, no. 6 (2018): 4229-4241. [CrossRef]
37. Lee, Chul Joo, Seung Hyuk Kwon, Hyoung Jin Choi, Kyung Ho Chung, and Jae Heum Jung. "Enhanced magnetorheological performance of carbonyl iron/natural rubber composite elastomer with gamma-ferrite additive." Colloid and Polymer Science 296, no. 9 (2018): 1609-1613. [CrossRef]
38. Li, Y.; Li, J.; Li, W.; Samali, B. Development And Characterization Of A Magnetorheological Elastomer Based Adaptive Seismic Isolator. Smart Materials and Structures 2013, 22, 035005. [CrossRef]
39. Lee, C.; Kim, I.; Jung, H. Fabrication And Characterization Of Natural Rubber-Based Magnetorheological Elastomers At Large Strain For Base Isolators. Shock and Vibration 2018, 2018, 1-12. [CrossRef]
40. Cantournet, S.; Desmorat, R.; Besson, J. Mullins Effect And Cyclic Stress Softening Of Filled Elastomers By Internal Sliding And Friction Thermodynamics Model. International Journal of Solids and Structures 2009, 46, 2255-2264. [CrossRef]
41. Schubert, G.; Harrison, P. Large-Strain Behaviour Of Magneto-Rheological Elastomers Tested Under Uniaxial Compression And Tension, And Pure Shear Deformations. Polymer Testing 2015, 42, 122-134. [CrossRef]
42. Li, W.; Zhou, Y.; Tian, T. Viscoelastic Properties Of MR Elastomers Under Harmonic Loading. Rheologica Acta 2010, 49, 733-740. [CrossRef]
43. Ge, L.; Gong, X.; Fan, Y.; Xuan, S. Preparation And Mechanical Properties Of The Magnetorheological Elastomer Based On Natural Rubber/Rosin Glycerin Hybrid Matrix. Smart Materials and Structures 2013, 22, 115029. [CrossRef]
44. Kim, Y. K., Koo, J. H., Kim, K. S., & Kim, S. Vibration isolation strategies using magneto-rheological elastomer for a miniature cryogenic cooler in space application. In; 2010 IEEE/ASME International Conference on Advanced Intelligent Mechatronics: IEEE 2010; p. 1203-1206. [CrossRef]